



CMS-HIN-18-003

CERN-EP-2021-028
2021/02/26

Study of Drell–Yan dimuon production in proton-lead collisions at $\sqrt{s_{\text{NN}}} = 8.16 \text{ TeV}$

The CMS Collaboration^{*}

Abstract

Differential cross sections for the Drell–Yan process, including Z boson production, using the dimuon decay channel are measured in proton-lead (pPb) collisions at a nucleon-nucleon centre-of-mass energy of 8.16 TeV. A data sample recorded with the CMS detector at the LHC is used, corresponding to an integrated luminosity of 173 nb^{-1} . The differential cross section as a function of the dimuon mass is measured in the range 15–600 GeV, for the first time in proton-nucleus collisions. It is also reported as a function of dimuon rapidity over the mass ranges 15–60 GeV and 60–120 GeV, and ratios for the p-going over the Pb-going beam directions are built. In both mass ranges, the differential cross sections as functions of the dimuon transverse momentum p_T and of a geometric variable ϕ^* are measured, where ϕ^* highly correlates with p_T but is determined with higher precision. In the Z mass region, the rapidity dependence of the data indicate a modification of the distribution of partons within a lead nucleus as compared to the proton case. The data are more precise than predictions based upon current models of parton distributions.

Submitted to the Journal of High Energy Physics

1 Introduction

The annihilation of a quark-antiquark pair into two oppositely charged leptons, through the exchange of a Z boson or a virtual photon (Z/γ^*) in the s -channel, is known as the Drell-Yan (DY) process [1]. The theoretical derivation of the matrix elements is available up to next-to-next-to-leading order in perturbative quantum chromodynamics (QCD) with next-to-leading order (NLO) electroweak (EW) corrections [2–5]. A precise measurement of this process can add valuable information on its nonperturbative part, including the effect of parton distribution functions (PDFs) [6].

Measurements of EW bosons in proton-nucleus and nucleus-nucleus collisions probe the nuclear modification of the PDFs [7–10]. The presence of a nuclear environment has been long observed [11] to modify the parton densities in the nucleus, as compared to those in a free nucleon. A first-principle description of such (nonperturbative) nuclear effects remains an open challenge, but they can be modelled using nuclear PDFs (nPDFs) determined with data in the same collinear factorisation approach as for free protons. Global fits of nPDFs [12–19] predict a suppression for small longitudinal momentum fraction x , $x \lesssim 10^{-2}$ (i.e. shadowing [20] region), and an enhancement for intermediate x , $10^{-2} \lesssim x \lesssim 10^{-1}$ (i.e. antishadowing region).

Many measurements of the DY process, including the mass dependence, have been performed in proton-proton (pp) collisions, for instance by the ATLAS [21–25], CMS [26–30], and PHENIX [31] experiments. Measurements of the Z boson production have been performed in proton-lead (pPb) collisions by the ALICE [32, 33], ATLAS [34], and CMS [35] experiments, as functions of rapidity, transverse momentum, or centrality (related to the impact parameter of the collision).

In this paper, we report the measurement of the differential cross section for $\mu^+\mu^-$ production via the DY process, as a function of the following variables:

- dimuon mass, $m_{\mu\mu}$, in the interval $15 < m_{\mu\mu} < 600$ GeV;
- dimuon transverse momentum, p_T , in two dimuon mass intervals (15–60 GeV and 60–120 GeV, targeting the continuum at low mass and the Z boson, respectively);
- dimuon rapidity in the nucleon-nucleon centre-of-mass (CM) frame, y_{CM} , in the same two mass intervals; and
- ϕ^* [36–38] (defined below) in the same two mass intervals.

The dimuon mass and ϕ^* dependencies as well as cross sections in the dimuon mass range 15–60 GeV are reported for the first time in proton-nucleus collisions.

The variable ϕ^* , used in numerous Z boson studies, is defined as

$$\phi^* \equiv \tan\left(\frac{\pi - \Delta\phi}{2}\right) \sin(\theta_\eta^*), \quad (1)$$

where $\Delta\phi$ is the opening angle between the leptons, defined as the difference of their azimuthal angles in the plane transverse to the beam axis, and θ_η^* is related to the emission angle of the dilepton system with respect to the beam. The variable θ_η^* is defined in a frame that is Lorentz-boosted along the beam direction such that the two leptons are back-to-back in the transverse plane. This angle θ_η^* is related to the pseudorapidities of the leptons by the relation

$$\cos(\theta_\eta^*) = \tanh(\Delta\eta/2), \quad (2)$$

where $\Delta\eta$ is the difference in pseudorapidity between the two leptons. By construction, ϕ^* is greater than zero. This quantity strongly correlates with the dimuon p_T , while only depending

on angular quantities for the leptons. Thus, it is measured with better precision than p_T , especially at low p_T values. Since $\phi^* \sim p_T/m$, where m is the mass of the dilepton system, the range $\phi^* < 1$ corresponds to dilepton p_T up to about 100 GeV for a dilepton mass close to that of the Z boson.

The outline of this paper is as follows. In Section 2, the experimental methods are described, from the data and simulation samples used, up to the data analysis description and systematic uncertainties estimation. Results are presented and discussed in Section 3, before the summary in Section 4.

2 Experimental methods

2.1 Data taking conditions and the CMS detector

The results reported in this paper use pPb collision data taken by CMS at the end of 2016, at a nucleon-nucleon CM energy of $\sqrt{s_{\text{NN}}} = 8.16$ TeV at the CERN LHC. The total integrated luminosity corresponds to $173.4 \pm 6.1 \text{ nb}^{-1}$ [39]. In the first part of the pPb run, corresponding to $63 \pm 2 \text{ nb}^{-1}$, the proton beam was heading toward negative η , according to the CMS detector convention [40], with an energy of 6.5 TeV, and colliding with a lead nucleus beam with an energy of 2.56 TeV per nucleon. The beams were swapped for the second part of the run, corresponding to $111 \pm 4 \text{ nb}^{-1}$. Because of the asymmetric collision system, massless particles produced in the nucleon-nucleon CM frame at a given η_{CM} are reconstructed at $\eta_{\text{lab}} = \eta_{\text{CM}} - 0.465$ in the laboratory frame used in this paper, in which the proton is heading toward positive η . The measurements presented here are expressed in terms of η_{CM} .

The central feature of the CMS apparatus is a superconducting solenoid of 6 m internal diameter, providing a magnetic field of 3.8 T. Within the solenoid volume are a silicon pixel and strip tracker, a lead tungstate crystal electromagnetic calorimeter (ECAL), and a brass and scintillator hadron calorimeter (HCAL), each composed of a barrel and two endcap sections. Forward calorimeters extend the η coverage provided by the barrel and endcap detectors. The hadron forward (HF) calorimeter uses steel as the absorber and quartz fibres as the sensitive material. The two halves of the HF are located 11.2 m from the interaction region, one on each end, and together they provide coverage in the range $3.0 < |\eta| < 5.2$. They also serve as luminosity monitors. Muons are measured in the range $|\eta| < 2.4$ in gas-ionisation chambers embedded in the steel flux-return yoke outside the solenoid, with detection planes made using three technologies: drift tubes, cathode strip chambers, and resistive-plate chambers.

Events of interest are selected using a two-tiered trigger system. The first level, composed of custom hardware processors, uses information from the calorimeters and muon detectors to select events at a rate of around 100 kHz within a fixed latency of about $4 \mu\text{s}$ [41]. The second level, known as the high-level trigger (HLT), consists of a farm of processors running a version of the full event reconstruction software optimised for fast processing, and reduces the event rate to around 1 kHz (up to around 20 kHz during the pPb data taking) before data storage [42].

The reconstructed vertex with the largest value of summed physics-object p_T^2 is taken to be the primary pPb interaction vertex. The physics objects are the jets, clustered using the jet finding algorithm [43, 44] with the tracks assigned to the vertex as inputs, and the associated missing transverse momentum, taken as the negative vector sum of the p_T of those jets. During the data taking, the average number of collisions per bunch crossing was 0.18. The stability of the results has been checked against different such average number conditions.

The particle-flow algorithm [45] aims to reconstruct and identify each individual particle in an

event, with an optimised combination of information from the various elements of the CMS detector. The energy of photons is obtained from the ECAL measurement. The energy of electrons is determined from a combination of the electron momentum at the primary interaction vertex as determined by the tracker, the energy of the corresponding ECAL cluster, and the energy sum of all bremsstrahlung photons spatially compatible with originating from the electron track. The energy of muons is obtained from the curvature of the corresponding track. The energy of charged hadrons is determined from a combination of their momentum measured in the tracker and the matching ECAL and HCAL energy deposits, corrected for zero-suppression effects and for the response function of the calorimeters to hadronic showers. Finally, the energy of neutral hadrons is obtained from the corresponding corrected ECAL and HCAL energies.

Matching muons to tracks measured in the silicon tracker results in a relative transverse momentum resolution, for muons with p_T up to 100 GeV, of 1% in the barrel and 3% in the endcaps. The p_T resolution in the barrel is better than 7% for muons with p_T up to 1 TeV [46].

A more detailed description of the CMS detector, together with a definition of the coordinate system used and the relevant kinematic variables, can be found in Ref. [40].

2.2 Simulated samples

The signal and most backgrounds are modelled using Monte Carlo (MC) simulated samples. The following processes are considered: DY to $\mu^+\mu^-$ (signal) and to $\tau^+\tau^-$ (treated as background), $t\bar{t}$, diboson (WW, WZ, and ZZ), and single top quark production (tW and $\bar{t}W$, collectively referred to as tW in the paper). Additional MC samples are used, for the production of W bosons (decaying to muon and neutrino, or τ lepton and neutrino) and QCD multijet events. These backgrounds are estimated using control samples in data, as described later in the text, and the MC samples are only used for complementary studies.

The DY, W boson, $t\bar{t}$, and tW MC samples are generated using the NLO generator POWHEG v2 [47–50], modified to account for the mixture of proton-proton and proton-neutron interactions occurring in pPb collisions. The CT14 [51] PDF set is used, with nuclear modifications from EPPS16 [14] for the lead nucleus. Parton showering is performed by PYTHIA 8.212 [52] with the CUETP8M1 underlying event (UE) tune [53]. The decay of τ leptons in the $W \rightarrow \tau\nu_\tau$ MC samples is handled in POWHEG using TAUOLA 1.1.5 [54], including final-state radiative (FSR) quantum electrodynamics corrections using PHOTOS 2.15 [55]. The diboson and QCD multijet samples are generated at leading order using PYTHIA.

The aforementioned event generators only simulate single proton-nucleon interactions, with the proportion of protons and neutrons found in Pb nuclei. To consider a more realistic distribution of the UE present in pPb collisions, simulated events are embedded into two separate samples of minimum bias (MB) events generated with EPOS LHC (v3400) [56], one for each pPb boost direction. The EPOS MC samples provide a good description of the global event properties of the MB pPb data, such as the η distributions of charged hadrons [57] and the transverse energy density [58].

A difference is found between the dimuon p_T in POWHEG MC and that observed in data. To improve the modelling in the simulation, the POWHEG Z/γ^* samples are reweighted event-by-event using an empirical function of the generated boson p_T . This weight is applied in Z/γ^* MC samples in the derivation of the various corrections described below. However, it is not applied in the figures of this paper, where the original p_T spectrum from POWHEG is used.

The full detector response is simulated for all MC samples, using GEANT4 [59], with alignment and calibration conditions tuned to match collision data, and a realistic description of the beam

spot. The trigger decisions are also emulated, and the MC events are reconstructed with the standard CMS pp reconstruction algorithms used for the 2016 data.

The Z/γ^* , W , and $t\bar{t}$ samples are normalised to their NLO cross sections provided by POWHEG for pPb collisions, including EPPS16 modifications. The diboson samples are normalised to the cross sections measured by the CMS Collaboration in pp collisions at $\sqrt{s} = 8$ TeV [60–62]. The small difference in CM energy with the pPb data is covered by the data-driven correction described in Section 2.4 and smaller than the associated systematic uncertainty. The $t\bar{t}$ background is normalised to the CMS measurement in pPb collisions at $\sqrt{s_{\text{NN}}} = 8.16$ TeV [63]. All backgrounds receive a correction based on control samples in data, as described in Section 2.4.

Simulated events do not feature the same event activity (charged-particle multiplicity or energy density) as the data, mostly because selecting two energetic muons favours higher-activity events (with a larger number of binary nucleon-nucleon collisions), while the EPOS sample used for embedding simulates MB events. To ensure a proper description of event activity in simulation, the distribution of the energy deposited in both sides of the HF calorimeter is reweighted event-by-event so that it matches that observed in data (selecting $Z \rightarrow \mu^+\mu^-$ events). The corresponding weights have a standard deviation of 0.27 for a mean of 1.

2.3 Object reconstruction and event selection

The events used in the analysis are selected with a single-muon trigger, requiring $p_T > 12$ GeV for the muon reconstructed by the HLT. During both online and offline muon reconstruction, the data from the muon detectors are matched and fitted to data from the silicon tracker to form muon candidates. Each muon is required to be within the geometrical acceptance of the detector, $|\eta_{\text{lab}}| < 2.4$. The leading muon (with highest p_T) is matched to the HLT trigger object and is required to have $p_T > 15$ GeV, in the plateau of the trigger efficiency (around 95%, depending on η_{lab}). A looser selection of $p_T > 10$ GeV is applied to the other muon.

Muons are selected by applying the standard “tight” selection criteria [46] used, e.g. in Refs. [63, 64], with an efficiency of about 98%. Requirements on the impact parameter and the opening angle between the two muons are further imposed to reject cosmic ray muons. Events are selected for further analysis if they contain pairs of oppositely charged muons meeting the above requirements. The χ^2 divided by the number of degrees of freedom (dof) from a fit to the dimuon vertex must be smaller than 20, ensuring that the two muon tracks originate from a common vertex, thus reducing the contribution from heavy-flavour meson decays. In the rare events (about 0.4%) where more than one selected dimuon pair is found, the candidate with the smallest dimuon vertex χ^2 is kept.

To further suppress the background contributions due to muons originating from light and heavy flavour hadron decays, muons are required to be isolated, based on the p_T sum of the charged-particle tracks around the muon. Isolation sums are evaluated in a circular region of the (η, ϕ) plane around the lepton candidate with $\Delta R < 0.3$, where $\Delta R = \sqrt{(\Delta\eta)^2 + (\Delta\phi)^2}$. The relative isolation I_{rel} , obtained by dividing this isolation sum by the muon p_T , is required to be below 0.2.

In addition to the DY process, lepton pairs can also be produced through photon interactions. Exclusive coherent photon-induced dilepton production is enhanced in pPb collisions compared to pp data, because of the large charge of the lead nucleus. Hadronic collisions are selected by requiring at least one HF calorimeter tower with more than 3 GeV of total energy on either side of the interaction point. In order to further suppress the photon-induced background, characterised by almost back-to-back muons, events are required to contain at least

one additional reconstructed track, which completely removes this background. Incoherent photon-induced dimuon production, where the photon is emitted from a parton instead of the whole nucleus and amounting to less than 5% of the total dilepton cross section according to studies in pp collisions at $\sqrt{s} = 13\text{ TeV}$ [29, 65], is considered part of the signal and is neither removed nor subtracted.

2.4 Background estimation

Various backgrounds are estimated using one of the techniques described below, depending on the nature of the respective background process. Processes involving two isolated muons, such as $Z/\gamma^* \rightarrow \tau^+\tau^-$, $t\bar{t}$, tW , and dibosons, are estimated from simulation and corrected using the “ $e\mu$ method”. Processes with one or more muons in jets, namely $W+\text{jets}$ and multijet, are estimated using the “misidentification rate method”.

The $e\mu$ method takes advantage of the fact that the EW backgrounds, as opposed to the $Z/\gamma^* \rightarrow \mu^+\mu^-$ signal, also contribute to the $e\mu$ final state. Events with exactly one electron and one muon of opposite charge are used, where the muon is selected as described previously, matched to the HLT trigger muon and with $p_T > 15\text{ GeV}$, while the electron [66] must have $p_T > 20\text{ GeV}$ and fulfil the same isolation requirement as the muon. The small contribution from heavy-flavour meson decays is estimated from same-sign $e\mu$ events. The data-to-simulation ratio with this selection, in each bin of the measured variables, is used to correct the simulated samples in the $\mu^+\mu^-$ final state. This ratio is compatible with unity in most bins.

The misidentification rate method estimates the probability for a muon inside a jet and passing the tight selection criteria to pass the isolation requirements. This probability (the misidentification rate) is estimated as a function of p_T , separately for $|\eta_{\text{lab}}| < 1.2$ and $|\eta_{\text{lab}}| > 1.2$. A sideband in data is selected from opposite-sign dimuon events in which the dimuon vertex χ^2 selection has been inverted. This sample is dominated by contributions from multijet and $W+\text{jets}$ production, and the small contribution from EW processes, estimated using simulation, is removed. The misidentification rate is then applied to a control dimuon data sample, passing the dimuon vertex χ^2 selection but in which neither of the two muons passes the isolation requirement, to obtain the multijet contribution in the signal region, where both muons are isolated. The $W+\text{jets}$ contribution is estimated with a similar procedure, using events in which exactly one of the two muons passes the isolation requirement. The small contribution from EW processes to these control data samples is estimated using simulation and removed. The multijet contribution in the sample with exactly one isolated muon is also accounted for, using the same technique. The validity of this method is checked in a control sample of same-sign dimuon data, which is also dominated by the multijet and $W+\text{jets}$ processes. The same-sign data are found to be compatible with the predictions from the misidentification rate method in most bins, and the residual difference is accounted for as a systematic uncertainty.

In Figs. 1 and 2, data are compared to the prediction from DY simulation and background expectations estimated using the techniques described above. A good overall agreement is found between the data and the expectation, which is dominated by the DY signal. Some hints for the differences will be discussed in terms of potential physics implications in Section 3: they include data above expectation for $m_{\mu\mu} < 50\text{ GeV}$, as well as for $y_{\text{CM}} > 0$ when $60 < m_{\mu\mu} < 120\text{ GeV}$, and trends in dimuon p_T and ϕ^* , as mentioned in Section 2.2.

2.5 Muon momentum scale and resolution corrections

The muon momentum scale and resolution are corrected in both data and simulation following the standard CMS procedure described in Ref. [67]. These corrections have been derived using

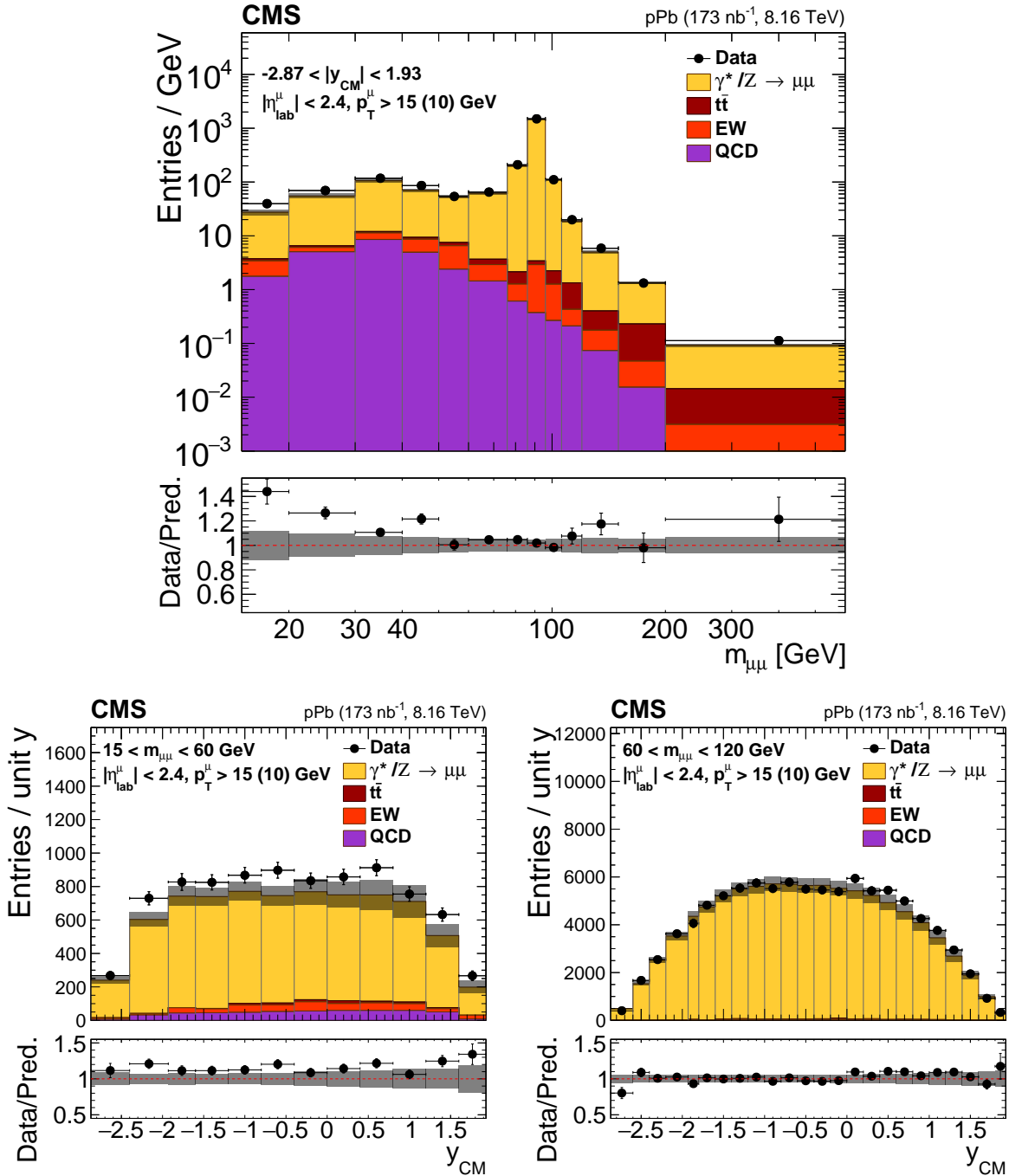


Figure 1: Comparison of the data (black points) with the Z/γ^* signal and background expectations (filled histograms, where "EW" includes $Z/\gamma^* \rightarrow \tau^+\tau^-$ and diboson), estimated as described in the text, as a function of invariant mass (upper) and rapidity in the centre-of-mass frame for $15 < m_{\mu\mu} < 60 \text{ GeV}$ (lower left) and $60 < m_{\mu\mu} < 120 \text{ GeV}$ (lower right). Vertical error bars represent statistical uncertainties. The ratios of data over expectations are shown in the lower panels. The boson p_T reweighting described in the text is not applied. The shaded regions show the quadratic sum of the systematic uncertainties (including the integrated luminosity, but excluding acceptance and unfolding uncertainties) and the nPDF uncertainties (CT14+EPPS16).

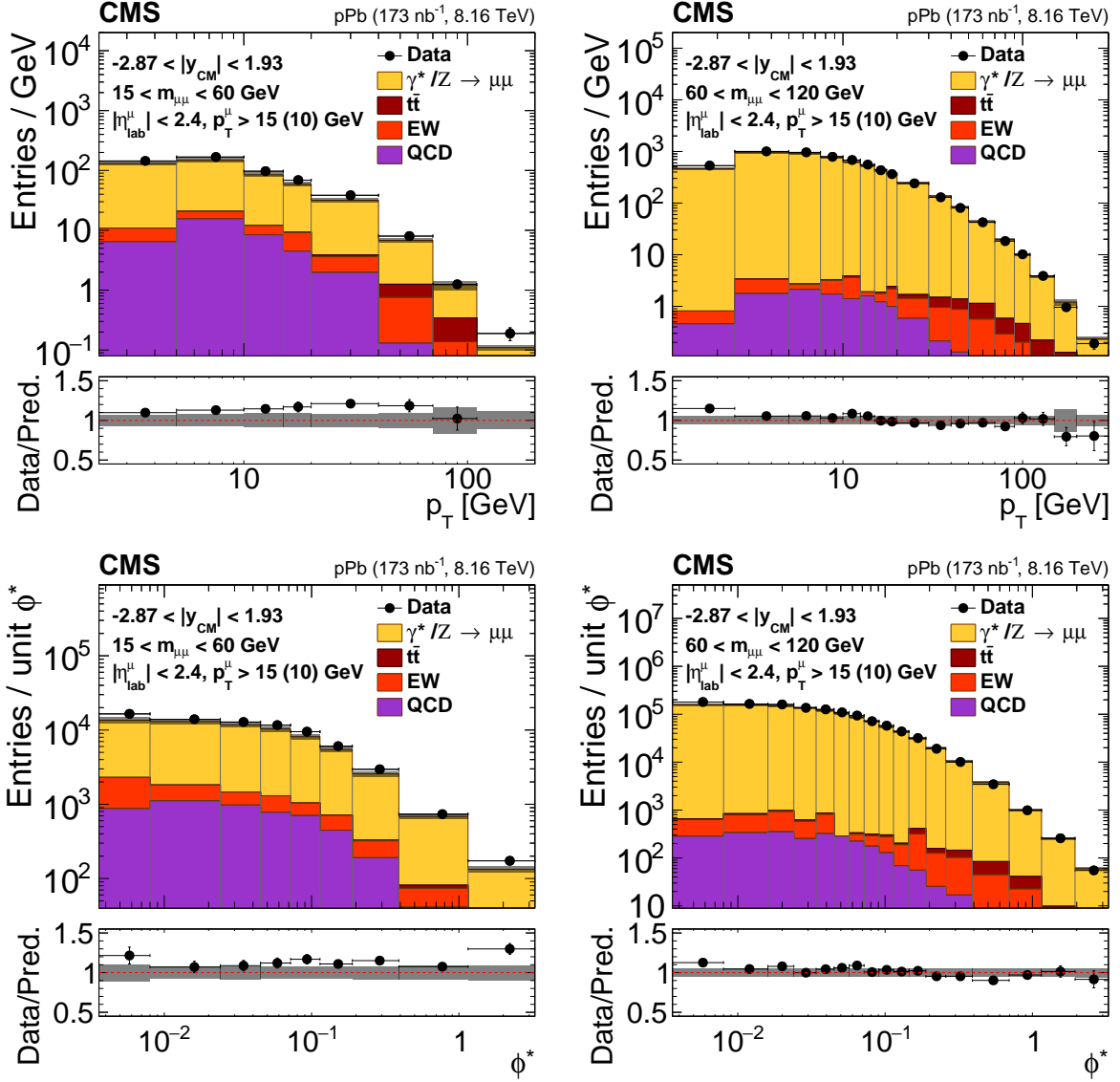


Figure 2: Comparison of the data (black points) with the Z/γ^* signal and background expectations (filled histograms, where "EW" includes $Z/\gamma^* \rightarrow \tau^+\tau^-$ and diboson), estimated as described in the text, as a function of p_T (upper row) and ϕ^* (lower row), for $15 < m_{\mu\mu} < 60 \text{ GeV}$ (left) and $60 < m_{\mu\mu} < 120 \text{ GeV}$ (right). The first bins of the p_T and ϕ^* distributions start at 0. Vertical error bars represent statistical uncertainties. The ratios of data over expectations are shown in the lower panels. The boson p_T reweighting described in the text is not applied. The shaded regions show the quadratic sum of the systematic uncertainties (including the integrated luminosity, but excluding acceptance and unfolding uncertainties) and the nPDF uncertainties (CT14+EPPS16).

the pp data sample at $\sqrt{s} = 13$ TeV recorded in 2016, with the same detector conditions as the pPb data set used in the present analysis.

In addition, the measurement is unfolded to account for finite momentum resolution. No regularisation is found to be needed given the good resolution and modest migrations between the analysis bins, and the maximum likelihood estimate [68] (obtained from the inversion of the response matrix, derived using simulated NLO POWHEG samples) is used to obtain the unfolded results. The effect of the unfolding is less than 1% in most cases, except for the mass dependence close to the Z boson mass peak, where it can amount to up to 15%.

2.6 Acceptance and efficiency

After subtraction of the contributions from different background processes, correction for the muon momentum resolution and scale, and unfolding for the detector resolution, the data need to be corrected for the acceptance and efficiency. The acceptance is defined as the fraction of generated signal events in the full phase space (within the quoted dimuon mass range and $-2.87 < y_{\text{CM}} < 1.93$) passing the kinematic selection defining the so-called fiducial region: leading muon $p_T > 15$ GeV, trailing muon $p_T > 10$ GeV, and $|\eta_{\text{lab}}| < 2.4$. Results are presented both with and without this acceptance correction, i.e. extrapolated to the full phase space and restricted to the fiducial region, respectively. The efficiency is the fraction of these events passing all other analysis selection criteria, including trigger selection, muon identification and isolation, and dimuon selection.

The efficiency is also checked in data, using Z boson events, with a *tag-and-probe* technique, as described in Ref. [69]. The same procedure and corrections are used as in the measurement of W^\pm bosons in pPb collisions [64]. The observed differences between the efficiency in data and simulation, estimated separately for the trigger, identification, and isolation, are accounted for as scale factors on a per-muon basis that are applied to the simulated events. These corrections are applied both in the efficiency estimation and in the construction of the background templates described in Section 2.4. When both muons in the event have $p_T > 15$ GeV, they can both pass the single-muon trigger used in this data analysis, and the scale factor is computed from the product of inefficiencies. For the muon and central track reconstruction, the data and MC simulation are found to give comparable efficiencies ($> 99.9\%$) and therefore no scale factor is applied for these two components of the efficiency.

2.7 Final-state radiation effects

Muons may undergo final-state radiation before being measured in the CMS detector, biasing their momentum and shifting the dimuon mass to lower values. We unfold the measured distributions, after efficiency correction (as well as acceptance, if applicable), to the “pre-FSR” quantities, used for the presentation of our results and defined from a “dressed lepton” definition [28]. Generator-level muon four-momenta are recalculated by adding the four-momenta of all generated photons found inside a cone of radius $\Delta R = 0.1$ around the muon. Again the response matrices for this unfolding procedure, derived using simulated NLO POWHEG samples, are found to be close to diagonal, thus no regularisation is needed in the unfolding.

2.8 Systematic uncertainties

Several sources of systematic uncertainties are evaluated. They are estimated in each bin of the measured distributions and added in quadrature. The list of systematic uncertainties is summarised in Table 1 and details of the estimation of each source are given below.

Theoretical uncertainties have an impact on the acceptance and efficiency. The renormalisation and factorisation scales have been varied from half to twice their nominal value (set to the dimuon mass), and the envelope of the variations, excluding combinations where both scales are varied in opposite directions, is taken as an uncertainty. In addition, the strong coupling constant value is varied by 0.0015 from its default value, $\alpha_S(m_Z) = 0.118$, as recommended by PDF4LHC [70]. The CT14 and EPPS16 uncertainties are also included, estimated with LHAPDF6 [71] using the PDF4LHC recommendations for Hessian (n)PDF sets [70]. Finally, the full difference between the acceptance and efficiency obtained with and without the Z boson p_T reweighting is considered as a systematic uncertainty. The impact of these uncertainties is less than 1% on the efficiency, but up to 10% on the acceptance for low dimuon masses.

We also include uncertainties stemming from the estimation of the efficiencies from data. The statistical component coming from the limited Z boson sample available is treated as a systematic uncertainty in this analysis. We also consider systematic effects associated with the choice of function used to model the p_T behaviour of the efficiencies, the dimuon mass fitting procedure to the Z boson peak in the extraction of the efficiencies, a possible data-to-simulation difference in the muon reconstruction efficiency, and the effect of the mismodelling in simulation of the event activity and for additional interactions per bunch crossing. The magnitude of these uncertainties ranges from 1 to 5% at low dimuon mass.

Regarding the estimation of EW backgrounds with the $e\mu$ method, the statistical uncertainty in the correction factors is included as a systematic uncertainty, as well as the effect of varying the $t\bar{t}$ cross section by its uncertainty, 18% [63], the uncertainty in the transfer factor for the heavy-flavour contribution, and the difference between the data and simulation in the $e\mu$ distributions. The systematic uncertainty in the multijet and W+jets backgrounds, related to the misidentification rate method, receives several contributions. The statistical uncertainty in the templates derived from data is accounted for, and combined with the full difference between the nominal estimation and an alternative method (based on a different sideband in data, using same-sign dimuon events). The residual nonclosure in the same-sign data sample, as well as its statistical uncertainty, are also both added in quadrature to the other uncertainties related to the misidentification rate method. The total systematic uncertainty in the background estimate, dominated by the residual nonclosure in most bins, ranges from less than 0.5 to 15% (for large dimuon p_T).

A different reweighting of the event activity in simulated samples is derived, as a function of the number of offline tracks reconstructed with $|\eta_{\text{lab}}| < 2.5$ instead of the nominal correction using the total energy deposited in the HF calorimeters, which modifies the efficiency and the background estimation. The observed difference in the measurements, which is less than 1% in most bins, is taken as a systematic uncertainty.

Uncertainties in the muon momentum scale and resolution corrections have been evaluated, based on the 2016 pp data sample at $\sqrt{s} = 13$ TeV, from which they are derived. These uncertainties, about 1% or less, arise from the limited data sample size available and variations in the method and its assumptions.

Response matrices used in the muon momentum scale and FSR unfoldings have been recalculated using the first and second parts of the run alone (accounting for statistical uncertainties in simulation), and using the PYQUEN generator v1.5.1 [72] instead of POWHEG (for a conservative estimation of the model dependence). Differences in the unfolded results, which are up to 2%, are taken into account as a systematic uncertainty.

Finally, the uncertainty in the integrated luminosity measurement is 3.5% [39].

Table 1: Range of systematic uncertainties in percentage of the cross section, given separately for $15 < m_{\mu\mu} < 60$ and $60 < m_{\mu\mu} < 120$ GeV. Systematic uncertainties for the three mass bins above 120 GeV fall in the range given for $15 < m_{\mu\mu} < 60$ GeV. For the theoretical component of acceptance and efficiency, the systematic uncertainty related to efficiency alone (for fiducial cross sections) is given between parentheses.

Source of uncertainty	$15 < m_{\mu\mu} < 60$ GeV	$60 < m_{\mu\mu} < 120$ GeV
Event activity reweighting	<3%	<1%
Muon momentum	<1%	<3%
Data-driven efficiencies	1–5%	1–4%
Acceptance and efficiency (MC stat.)	<4%	<4%
Background estimation	2–15%	0.1–3%
Acceptance and efficiency (theory)	1–10% (<1%)	<1% (<1%)
Unfolding: detector resolution	<2%	<2%
Unfolding: FSR	<1%	<1%
Total	6–15%	1–12%

Correlations across bins of these uncertainties have also been evaluated. Theoretical uncertainties are assumed to be fully correlated, with the exception of the nPDF uncertainty, whose correlation is calculated using the CTEQ prescription for Hessian sets [73]. Systematic uncertainties in the efficiency scale factors obtained from control samples in data are assumed to be uncorrelated, since they could have different effects in different kinematic regions, while statistical correlations between the scale factors derived in the same region of the detector are accounted for. No correlation is assumed for the uncertainties related to the background estimation. Uncertainties related to the HF energy reweighting, unfolding, and integrated luminosity are treated as fully correlated between the bins and measurements, as well as each of the sources of uncertainty in the muon momentum scale and resolution corrections. The correlation matrices for systematic uncertainties are shown in Figs. 3 and 4, excluding the fully correlated integrated luminosity uncertainty for clarity. They are derived from the total covariance matrix, obtained from the sum of the covariance matrices for the individual sources, assuming the correlations above. For a given variable, the difference between the matrices in the two mass selections can be explained by the background uncertainty, which is one of the dominant systematic uncertainties for $15 < m_{\mu\mu} < 60$ GeV but negligible most of the time for $60 < m_{\mu\mu} < 120$ GeV, except at large p_T or ϕ^* .

3 Results and discussion

Fiducial cross section results, where the fiducial volume is defined from the single-muon p_T and η_{lab} selection, are shown in Figs. 5 and 6, as functions of the dressed lepton kinematic variables (as discussed in Section 2.7), together with the expectations from POWHEG, using the CT14 [51] or CT14+EPPS16 [14] PDF sets. Cross sections in the full phase space, $-2.87 < y_{\text{CM}} < 1.93$, i.e. including the acceptance correction for the single-muon kinematic selections, are presented in Figs. 7 and 8.

The CT14+EPPS16 predictions suffer from a larger uncertainty than CT14 alone, which is coming from the parametrisation of the nuclear modification of the PDFs. Since the dimuon rapidity is strongly correlated with the longitudinal momentum fraction x_{Pb} of the parton in the lead nucleus, one can identify the shadowing region in the rapidity dependence of the cross

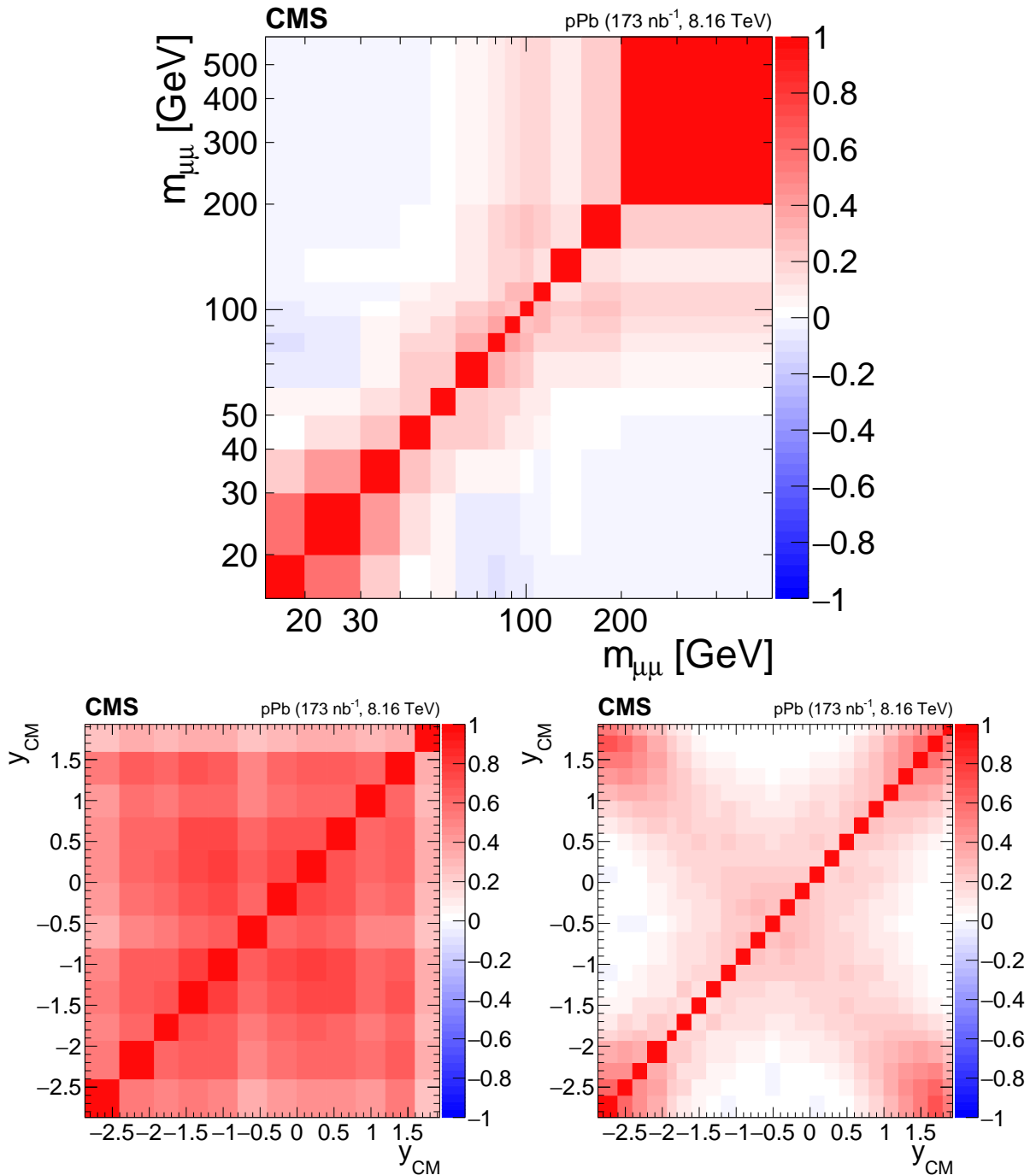


Figure 3: Correlation matrix for the systematic uncertainties, excluding integrated luminosity, as a function of the dimuon invariant mass (upper) and rapidity in the centre-of-mass frame for $15 < m_{\mu\mu} < 60 \text{ GeV}$ (lower left) and $60 < m_{\mu\mu} < 120 \text{ GeV}$ (lower right).

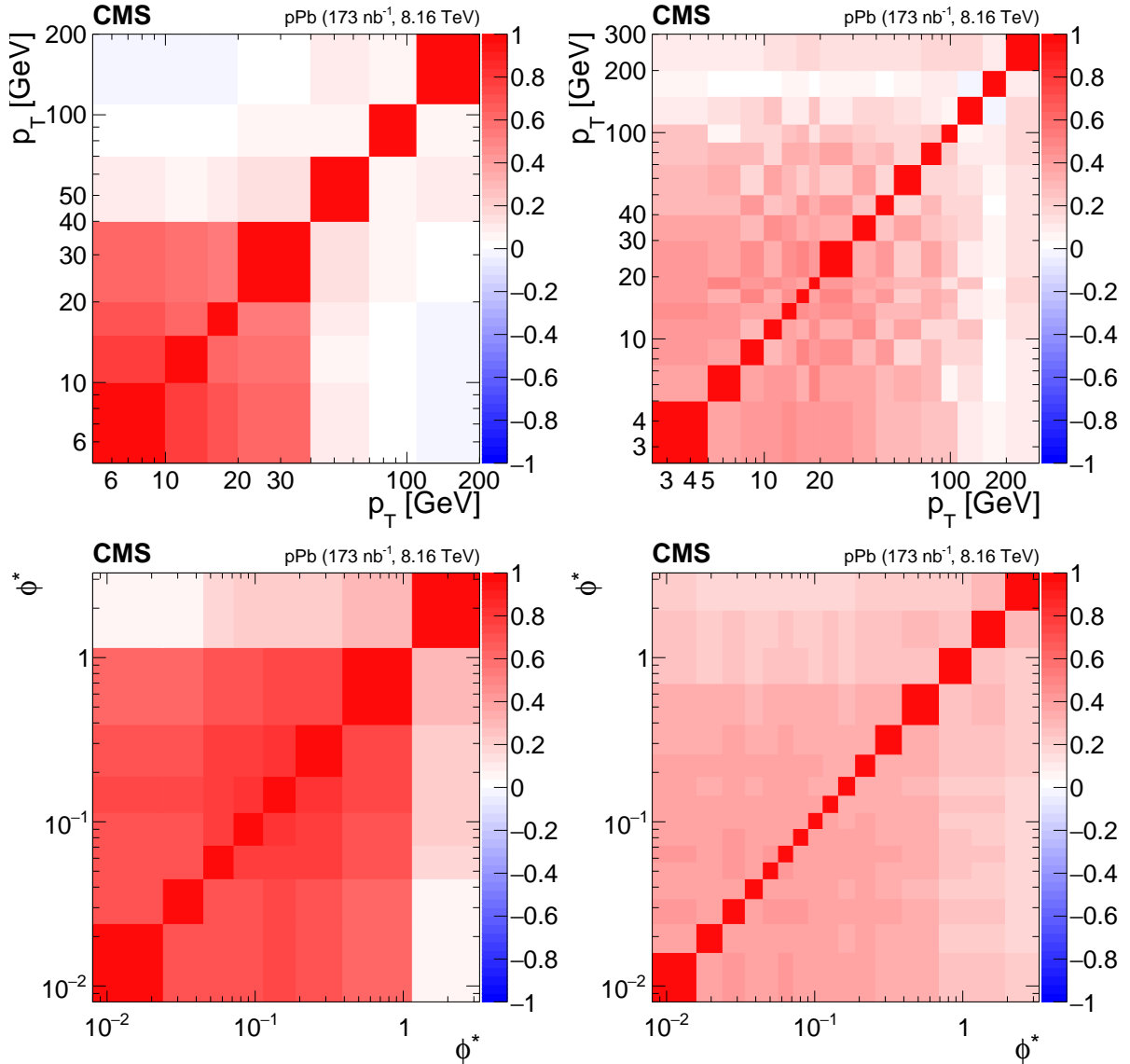


Figure 4: Correlation matrices for the systematic uncertainties, excluding integrated luminosity, as functions of p_T (upper row) and ϕ^* (lower row), for $15 < m_{\mu\mu} < 60$ GeV (left) and $60 < m_{\mu\mu} < 120$ GeV (right).

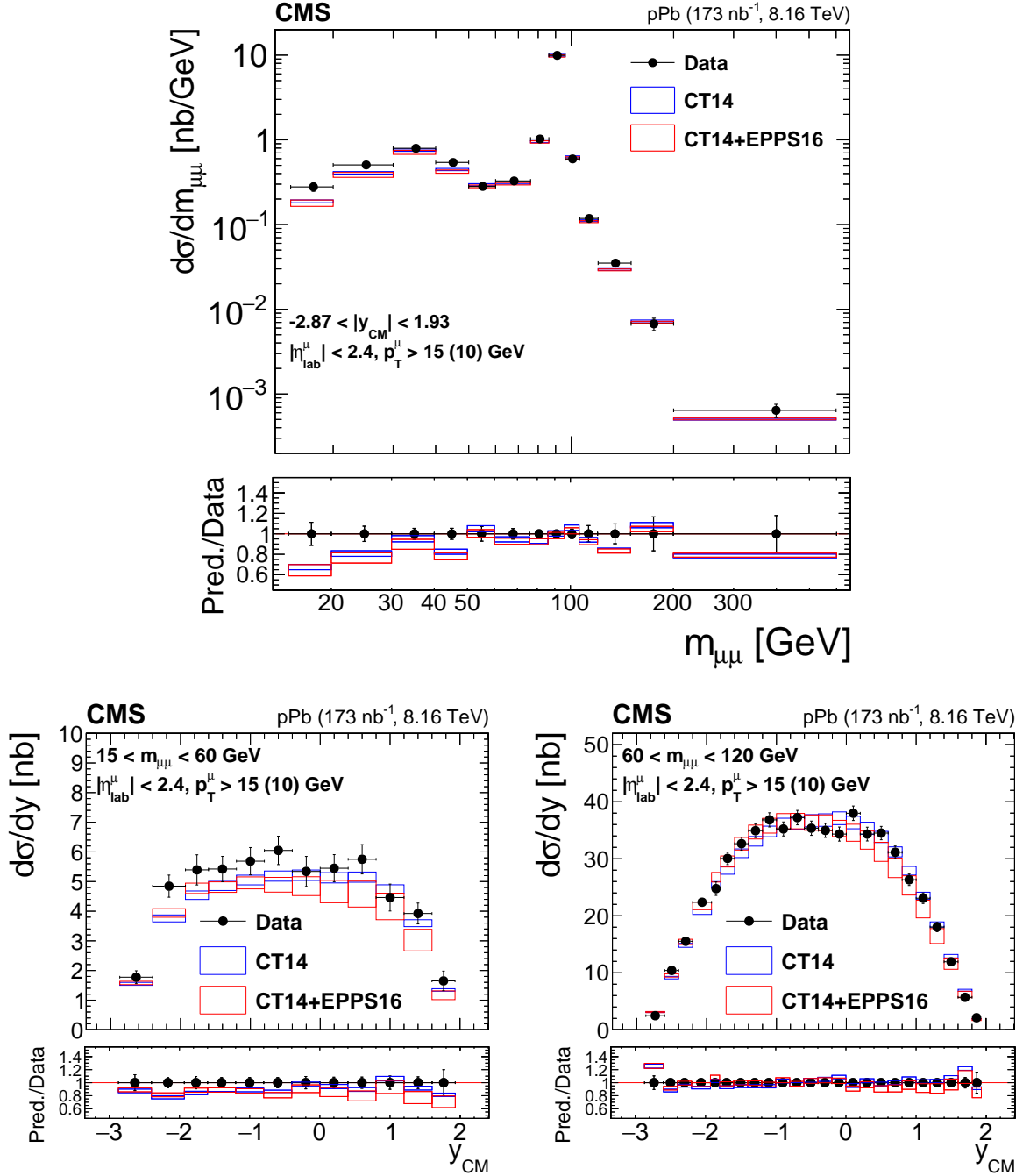


Figure 5: Differential fiducial cross section (without the acceptance correction) for the DY process measured in the muon channel, as a function of the dimuon invariant mass (upper) and rapidity in the centre-of-mass frame for $15 < m_{\mu\mu} < 60 \text{ GeV}$ (lower left) and $60 < m_{\mu\mu} < 120 \text{ GeV}$ (lower right). The error bars on the data represent the quadratic sum of the statistical and systematic uncertainties. Theory predictions from the POWHEG NLO generator are also shown, using CT14 (blue) or CT14+EPPS16 (red). The boxes show the 68% confidence level (n)PDF uncertainty on these predictions. The ratios of predictions over data are shown in the lower panels, where the data and (n)PDF uncertainties are shown separately, as error bars around one and as coloured boxes, respectively.

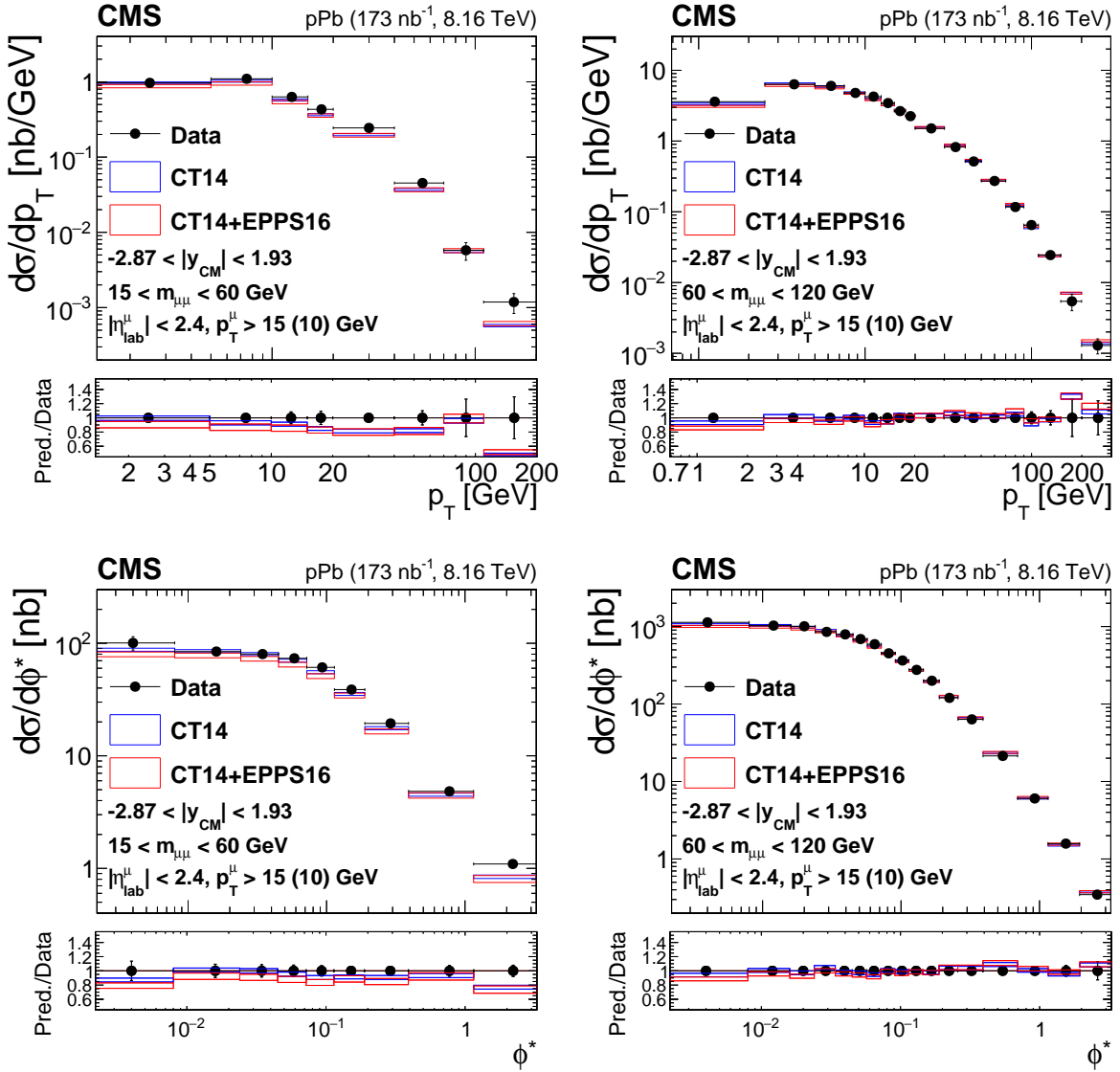


Figure 6: Differential fiducial cross sections (without the acceptance correction) for the DY process measured in the muon channel, as functions of p_T (upper row) and ϕ^* (lower row), for $15 < m_{\mu\mu} < 60$ GeV (left) and $60 < m_{\mu\mu} < 120$ GeV (right). The first bin of the p_T and ϕ^* measurements starts at 0. The error bars on the data represent the quadratic sum of the statistical and systematic uncertainties. Theory predictions from the POWHEG NLO generator are also shown, using CT14 (blue) or CT14+EPPS16 (red). The boxes show the 68% confidence level (n)PDF uncertainty on these predictions. The ratios of predictions over data are shown in the lower panels, where the data and (n)PDF uncertainties are shown separately, as error bars around one and as coloured boxes, respectively.

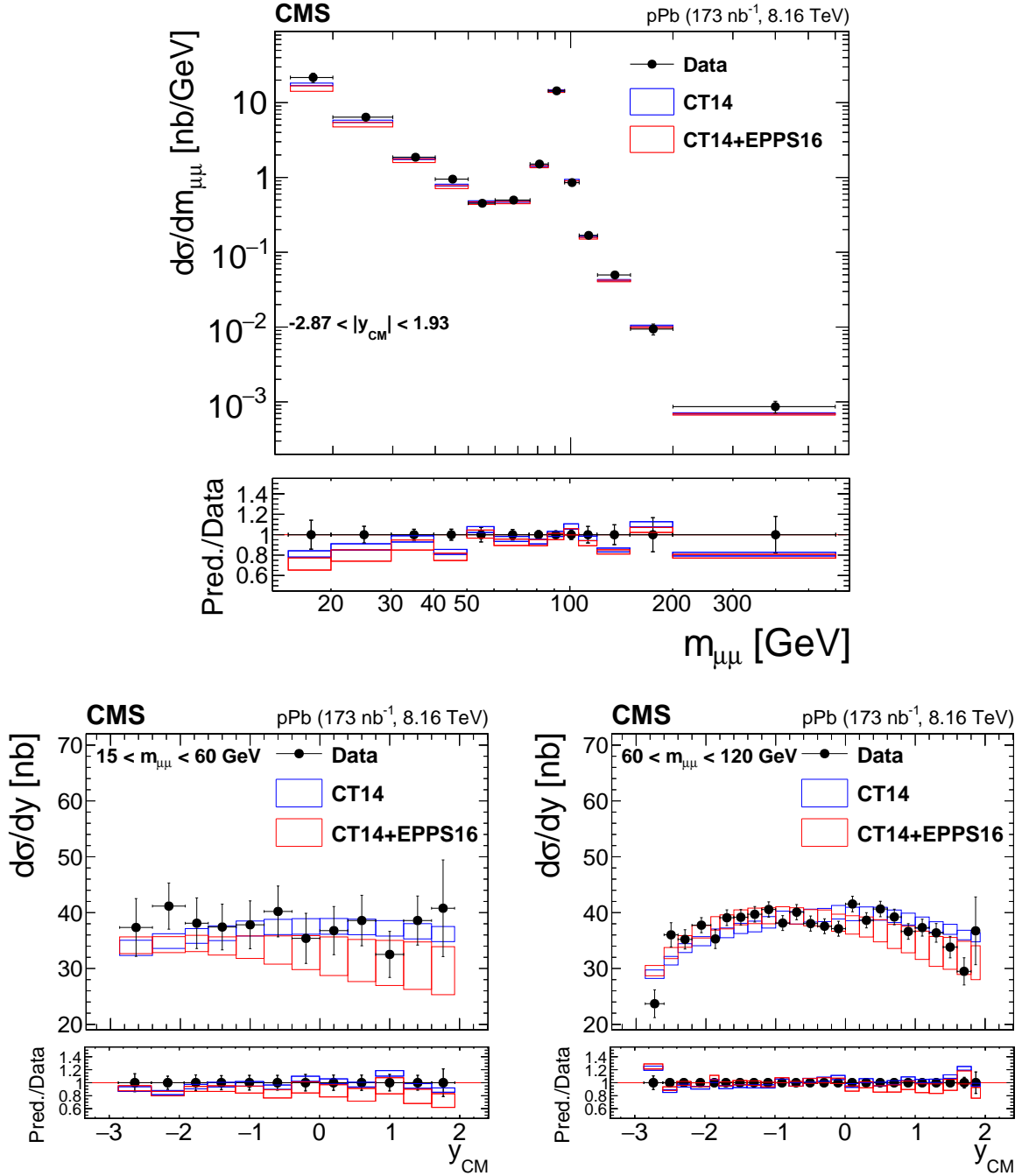


Figure 7: Differential cross section for the DY process measured in the muon channel, as a function of the dimuon invariant mass (upper) and rapidity in the centre-of-mass frame for $15 < m_{\mu\mu} < 60 \text{ GeV}$ (lower left) and $60 < m_{\mu\mu} < 120 \text{ GeV}$ (lower right). The error bars on the data represent the quadratic sum of the statistical and systematic uncertainties. Theory predictions from the POWHEG NLO generator are also shown, using CT14 (blue) or CT14+EPPS16 (red). The boxes show the 68% confidence level (n)PDF uncertainty on these predictions. The ratios of predictions over data are shown in the lower panels, where the data and (n)PDF uncertainties are shown separately, as error bars around one and as coloured boxes, respectively.

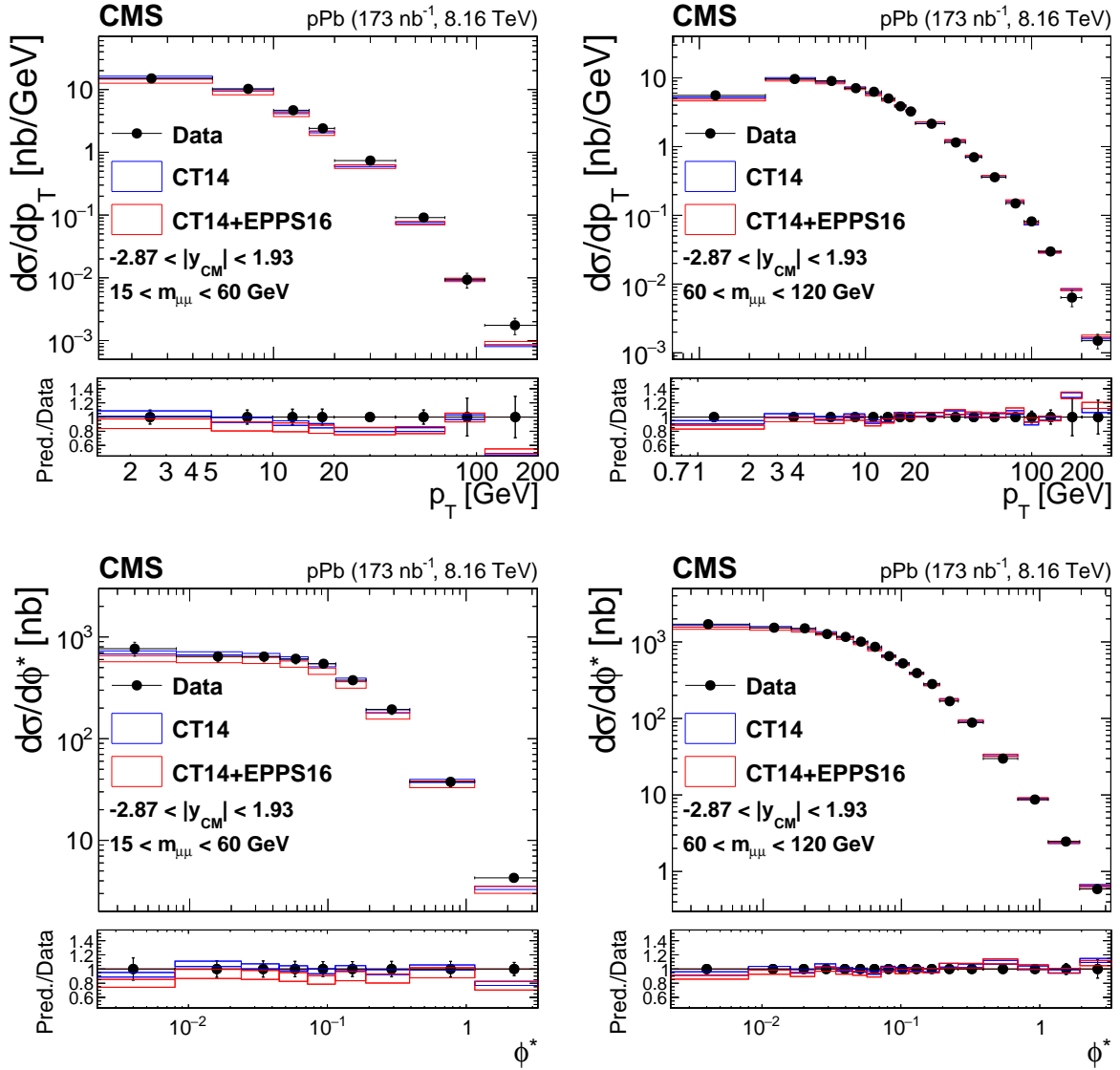


Figure 8: Differential cross sections for the DY process measured in the muon channel, as functions of p_T (upper row) and ϕ^* (lower row), for $15 < m_{\mu\mu} < 60 \text{ GeV}$ (left) and $60 < m_{\mu\mu} < 120 \text{ GeV}$ (right). The first bin of the p_T and ϕ^* measurements starts at 0. The error bars on the data represent the quadratic sum of the statistical and systematic uncertainties. Theory predictions from the POWHEG NLO generator are also shown, using CT14 (blue) or CT14+EPPS16 (red). The boxes show the 68% confidence level (n)PDF uncertainty on these predictions. The ratios of predictions over data are shown in the lower panels, where the data and (n)PDF uncertainties are shown separately, as error bars around one and as coloured boxes, respectively.

section, in the full measured rapidity range for $15 < m_{\mu\mu} < 60 \text{ GeV}$ and at positive rapidity for $60 < m_{\mu\mu} < 120 \text{ GeV}$. In the latter mass range, rapidities $y_{\text{CM}} \lesssim -1$ correspond to the antishadowing region. The inclusion of EPPS16 nuclear PDF modifications tends to provide a better description of the rapidity dependence in data for $60 < m_{\mu\mu} < 120 \text{ GeV}$ than the use of the CT14 PDF alone. Uncertainties in the measurement are also smaller than nPDF uncertainties in the Z boson mass region for most analysis bins, showing that these data will impose strong constraints if included in future nPDF fits.

The mass dependence of the cross section sheds further light on the shadowing effects probed at low mass, i.e. at lower x_{Pb} and lower scales than using Z bosons. The cross section measurement extends down to masses close to the Y meson masses, with potential implications in the understanding of the interplay between nPDF and other effects in quarkonium production in proton-nucleus collisions [74].

The difference between the fiducial cross sections, shown in Figs. 5 and 6, and the ones corrected to the full phase space, shown in Figs. 7 and 8, is largest for low masses. The absence of acceptance correction in the former results reduces their model dependence and corresponding theoretical uncertainty, making clearer the trend for a higher cross section in data for low dimuon masses compared to the POWHEG expectation.

The p_{T} and ϕ^* dependencies of the cross section, especially in the Z boson mass region, both point to a slight mismodelling in POWHEG, reminiscent of the trend reported previously [35], where the data are softer than POWHEG predictions. The large sensitivity of these observables to the details of the QCD model, especially nonperturbative effects, is also observed in pp collisions [30] and prevents one from using them to draw unambiguous conclusions about nPDFs. This precise measurement in pPb collisions provides new insight into the soft QCD phenomena dominating the production at low boson p_{T} or ϕ^* , and their possible modification with respect to pp collisions.

Integrated cross sections are also reported, in two mass ranges, in the fiducial region (fid.) or in the full phase space for $-2.87 < y_{\text{CM}} < 1.93$ (full):

$$\begin{aligned}\sigma(p\text{Pb} \rightarrow \gamma^*/Z \rightarrow \mu^+\mu^-, \text{fid.}, 15 < m_{\mu\mu} < 60 \text{ GeV}) &= 22.6 \pm 0.5 \text{ (stat)} \pm 0.8 \text{ (syst) nb}, \\ \sigma(p\text{Pb} \rightarrow \gamma^*/Z \rightarrow \mu^+\mu^-, \text{fid.}, 60 < m_{\mu\mu} < 120 \text{ GeV}) &= 122.3 \pm 0.9 \text{ (stat)} \pm 1.6 \text{ (syst) nb}, \\ \sigma(p\text{Pb} \rightarrow \gamma^*/Z \rightarrow \mu^+\mu^-, \text{full}, 15 < m_{\mu\mu} < 60 \text{ GeV}) &= 181.7 \pm 3.6 \text{ (stat)} \pm 14.4 \text{ (syst) nb}, \\ \sigma(p\text{Pb} \rightarrow \gamma^*/Z \rightarrow \mu^+\mu^-, \text{full}, 60 < m_{\mu\mu} < 120 \text{ GeV}) &= 177.7 \pm 1.3 \text{ (stat)} \pm 2.7 \text{ (syst) nb}.\end{aligned}$$

In Tables 2 and 3, the χ^2 values between the data and the predictions are reported, accounting for the bin-to-bin correlations for experimental (systematic uncertainties, shown in Figs. 3 and 4) and theoretical (from nPDF) uncertainties. The observations discussed above from Figs. 5 to 8 can be made here more quantitatively and more precisely with fiducial cross sections, thanks to the smaller systematic uncertainty. The inclusion of the EPPS16 modifications to the PDFs of the lead nucleus tends to improve the description for y_{CM} in the Z boson mass region, but conclusions are not clear for other quantities, and could even be opposite in the case of p_{T} and ϕ^* in that region. However, the manifestly imperfect modelling of the cross sections in POWHEG prevents from drawing strong conclusions about nPDFs using these variables.

Forward-backward ratios (R_{FB}) are built from the rapidity-dependent cross sections in the two mass regions, defined as the ratio of the $y_{\text{CM}} > 0$ to the $y_{\text{CM}} < 0$ cross sections (p-going to Pb-going). They are shown in Fig. 9. In both mass regions, the R_{FB} is by construction equal to unity in the absence of nuclear effect (CT14), but decreasing with $|y_{\text{CM}}|$ with CT14+EPPS16

Table 2: χ^2 values between the data and the POWHEG predictions and associated probability, from the fiducial cross sections, when experimental and theoretical bin-to-bin correlations are taken into account. The integrated luminosity uncertainty is included in the experimental uncertainties.

Observable	Mass range	χ^2	CT14			EPPS16		
			dof	Prob. [%]	χ^2	dof	Prob. [%]	
$m_{\mu\mu}$	$15 < m_{\mu\mu} < 600 \text{ GeV}$	35	13	0.10	30	13	0.42	
y_{CM}	$60 < m_{\mu\mu} < 120 \text{ GeV}$	51	24	0.12	35	24	6.6	
p_T	$60 < m_{\mu\mu} < 120 \text{ GeV}$	26	17	8.4	52	17	0.002	
ϕ^*	$60 < m_{\mu\mu} < 120 \text{ GeV}$	23	17	17	45	17	0.03	
y_{CM}	$15 < m_{\mu\mu} < 60 \text{ GeV}$	11	12	50	10	12	58	
p_T	$15 < m_{\mu\mu} < 60 \text{ GeV}$	12	8	15	8.5	8	38	
ϕ^*	$15 < m_{\mu\mu} < 60 \text{ GeV}$	8.3	9	50	9.0	9	44	

Table 3: χ^2 values between the data and the POWHEG predictions and associated probability, from the full phase space cross sections, when experimental and theoretical bin-to-bin correlations are taken into account. The integrated luminosity uncertainty is included in the experimental uncertainties.

Observable	Mass range	χ^2	CT14			EPPS16		
			dof	Prob. [%]	χ^2	dof	Prob. [%]	
$m_{\mu\mu}$	$15 < m_{\mu\mu} < 600 \text{ GeV}$	27	13	1.2	25	13	2.0	
y_{CM}	$60 < m_{\mu\mu} < 120 \text{ GeV}$	50	24	0.13	35	24	7.3	
p_T	$60 < m_{\mu\mu} < 120 \text{ GeV}$	28	17	4.5	51	17	0.003	
ϕ^*	$60 < m_{\mu\mu} < 120 \text{ GeV}$	25	17	9.3	44	17	0.03	
y_{CM}	$15 < m_{\mu\mu} < 60 \text{ GeV}$	7.4	12	83	6.0	12	92	
p_T	$15 < m_{\mu\mu} < 60 \text{ GeV}$	14	8	8.3	8.3	8	40	
ϕ^*	$15 < m_{\mu\mu} < 60 \text{ GeV}$	6.2	9	72	6.4	9	69	

and CT14+nCTEQ15WZ [19]. Similar conclusions are drawn as from the rapidity dependence of the cross section, but the construction of these ratios allows for the partial cancellation of theoretical and experimental uncertainties, accounting for the correlations described in the previous section. In particular, for $60 < m_{\mu\mu} < 120 \text{ GeV}$ and at large $|y_{\text{CM}}|$, an indication of a forward-backward ratio smaller than unity is found, consistent with the expectation from the combination of shadowing and antishadowing effects expected with CT14+EPPS16, as well as with similar results from W bosons [64]. Predictions using CT14+nCTEQ15WZ are found to be in good agreement with the data. The larger amount of shadowing in nCTEQ15 [15], hinted by the recent W boson measurement [64], is not predicted with nCTEQ15WZ. The low mass region is less conclusive, but nPDF uncertainties are smaller in this selection for nCTEQ15WZ than for EPPS16. Finally, experimental uncertainties for $60 < m_{\mu\mu} < 120 \text{ GeV}$ are smaller than the nPDF ones, once again showing relevance of these data to the study of nPDF effects.

4 Summary

Differential cross section measurements of the Drell–Yan process in the dimuon channel in proton-lead collisions at $\sqrt{s_{\text{NN}}} = 8.16 \text{ TeV}$ have been reported, including the transverse momentum (p_T) and rapidity dependencies in the Z boson mass region ($60 < m_{\mu\mu} < 120 \text{ GeV}$). In addition, for the first time in collisions including nuclei, the p_T and rapidity dependence for smaller masses $15 < m_{\mu\mu} < 60 \text{ GeV}$ have been measured. The dependence with ϕ^* (a

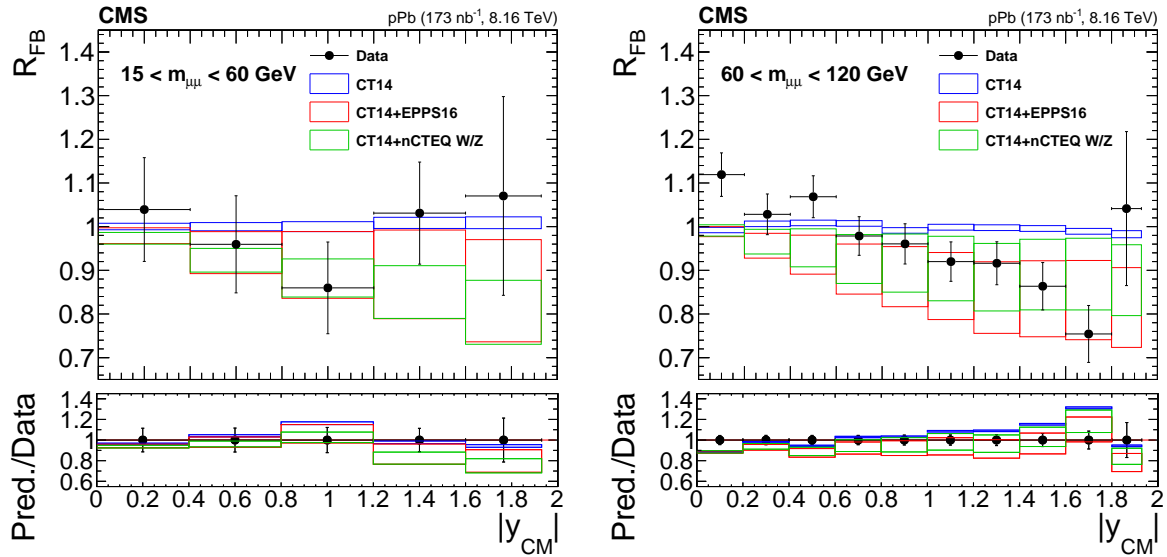


Figure 9: Forward-backward ratios for $15 < m_{\mu\mu} < 60 \text{ GeV}$ (left) and $60 < m_{\mu\mu} < 120 \text{ GeV}$ (right). The error bars on the data points represent the quadratic sum of the statistical and systematic uncertainties. The theory predictions from the POWHEG NLO generator are also shown, using CT14 [51] (blue), CT14+EPPS16 [14] (red), or CT14+nCTEQ15WZ [19] (green) PDF sets. The boxes show the 68% confidence level (n)PDF uncertainty in these predictions. The ratios of predictions over data are shown in the lower panels, where the data and the (n)PDF uncertainties are shown separately, as error bars around one and as coloured boxes, respectively.

geometrical variable that highly correlates with dimuon p_T but is determined with higher precision) for both $15 < m_{\mu\mu} < 60 \text{ GeV}$ and $60 < m_{\mu\mu} < 120 \text{ GeV}$ and the mass dependence from 15 to 600 GeV have been presented, also for the first time in proton-nucleus collisions. Finally, forward-backward ratios have been built from the rapidity-dependent cross sections for $y_{\text{CM}} > 0$ to $y_{\text{CM}} < 0$ in both mass regions, highlighting the presence of nuclear effects in the parton distribution functions.

Results for $60 < m_{\mu\mu} < 120 \text{ GeV}$ are the most precise to date, featuring smaller uncertainties than the theoretical predictions, and provide novel constraints on the quark and anti-quark nuclear parton distribution functions (nPDFs). Measurements in the lower mass range $15 < m_{\mu\mu} < 60 \text{ GeV}$ give access to a new phase space for nPDF studies, extending to lower longitudinal momentum fraction x and lower energy scale Q^2 . The p_T - and ϕ^* -dependent results are also very sensitive to the details of model details, such as soft quantum chromodynamics phenomena, which they may help to better understand in pPb collisions.

Acknowledgments

We congratulate our colleagues in the CERN accelerator departments for the excellent performance of the LHC and thank the technical and administrative staffs at CERN and at other CMS institutes for their contributions to the success of the CMS effort. In addition, we gratefully acknowledge the computing centres and personnel of the Worldwide LHC Computing Grid and other centres for delivering so effectively the computing infrastructure essential to our analyses. Finally, we acknowledge the enduring support for the construction and operation of the LHC, the CMS detector, and the supporting computing infrastructure provided by the

following funding agencies: BMBWF and FWF (Austria); FNRS and FWO (Belgium); CNPq, CAPES, FAPERJ, FAPERGS, and FAPESP (Brazil); MES (Bulgaria); CERN; CAS, MoST, and NSFC (China); COLCIENCIAS (Colombia); MSES and CSF (Croatia); RIF (Cyprus); SENESCYT (Ecuador); MoER, ERC PUT and ERDF (Estonia); Academy of Finland, MEC, and HIP (Finland); CEA and CNRS/IN2P3 (France); BMBF, DFG, and HGF (Germany); GSRT (Greece); NKFI (Hungary); DAE and DST (India); IPM (Iran); SFI (Ireland); INFN (Italy); MSIP and NRF (Republic of Korea); MES (Latvia); LAS (Lithuania); MOE and UM (Malaysia); BUAP, CINVESTAV, CONACYT, LNS, SEP, and UASLP-FAI (Mexico); MOS (Montenegro); MBIE (New Zealand); PAEC (Pakistan); MSHE and NSC (Poland); FCT (Portugal); JINR (Dubna); MON, RosAtom, RAS, RFBR, and NRC KI (Russia); MESTD (Serbia); SEIDI, CPAN, PCTI, and FEDER (Spain); MOSTR (Sri Lanka); Swiss Funding Agencies (Switzerland); MST (Taipei); ThEPCenter, IPST, STAR, and NSTDA (Thailand); TUBITAK and TAEK (Turkey); NASU (Ukraine); STFC (United Kingdom); DOE and NSF (USA).

Individuals have received support from the Marie-Curie programme and the European Research Council and Horizon 2020 Grant, contract Nos. 675440, 724704, 752730, and 765710 (European Union); the Leventis Foundation; the Alfred P. Sloan Foundation; the Alexander von Humboldt Foundation; the Belgian Federal Science Policy Office; the Fonds pour la Formation à la Recherche dans l’Industrie et dans l’Agriculture (FRIA-Belgium); the Agentschap voor Innovatie door Wetenschap en Technologie (IWT-Belgium); the F.R.S.-FNRS and FWO (Belgium) under the “Excellence of Science – EOS” – be.h project n. 30820817; the Beijing Municipal Science & Technology Commission, No. Z191100007219010; the Ministry of Education, Youth and Sports (MEYS) of the Czech Republic; the Deutsche Forschungsgemeinschaft (DFG), under Germany’s Excellence Strategy – EXC 2121 “Quantum Universe” – 390833306, and under project number 400140256 - GRK2497; the Lendület (“Momentum”) Programme and the János Bolyai Research Scholarship of the Hungarian Academy of Sciences, the New National Excellence Program ÚNKP, the NKFIA research grants 123842, 123959, 124845, 124850, 125105, 128713, 128786, and 129058 (Hungary); the Council of Science and Industrial Research, India; the Ministry of Science and Higher Education and the National Science Center, contracts Opus 2014/15/B/ST2/03998 and 2015/19/B/ST2/02861 (Poland); the National Priorities Research Program by Qatar National Research Fund; the Ministry of Science and Higher Education, project no. 0723-2020-0041 (Russia); the Programa Estatal de Fomento de la Investigación Científica y Técnica de Excelencia María de Maeztu, grant MDM-2015-0509 and the Programa Severo Ochoa del Principado de Asturias; the Thalis and Aristea programmes cofinanced by EU-ESF and the Greek NSRF; the Rachadapisek Sompot Fund for Postdoctoral Fellowship, Chulalongkorn University and the Chulalongkorn Academic into Its 2nd Century Project Advancement Project (Thailand); the Kavli Foundation; the Nvidia Corporation; the SuperMicro Corporation; the Welch Foundation, contract C-1845; and the Weston Havens Foundation (USA).

References

- [1] S. D. Drell and T.-M. Yan, “Massive lepton pair production in hadron-hadron collisions at high-energies”, *Phys. Rev. Lett.* **25** (1970) 316, doi:10.1103/PhysRevLett.25.316. [Erratum: doi:10.1103/PhysRevLett.25.902.2].
- [2] R. Hamberg, W. L. van Neerven, and T. Matsuura, “A complete calculation of the order α_s^2 correction to the Drell–Yan K-factor”, *Nucl. Phys. B* **359** (1991) 343, doi:10.1016/0550-3213(91)90064-5. [Erratum: doi:10.1016/S0550-3213(02)00814-3].

- [3] S. Catani et al., “Vector boson production at hadron colliders: a fully exclusive QCD calculation at next-to-next-to-leading order”, *Phys. Rev. Lett.* **103** (2009) 082001, doi:10.1103/PhysRevLett.103.082001, arXiv:0903.2120.
- [4] S. Catani and M. Grazzini, “Next-to-next-to-leading-order subtraction formalism in hadron collisions and its application to Higgs-boson production at the Large Hadron Collider”, *Phys. Rev. Lett.* **98** (2007) 222002, doi:10.1103/PhysRevLett.98.222002, arXiv:hep-ph/0703012.
- [5] K. Melnikov and F. Petriello, “Electroweak gauge boson production at hadron colliders through $O(\alpha_s^2)$ ”, *Phys. Rev. D* **74** (2006) 114017, doi:10.1103/PhysRevD.74.114017, arXiv:hep-ph/0609070.
- [6] A. D. Martin, W. J. Stirling, and R. G. Roberts, “Parton distributions of the proton”, *Phys. Rev. D* **50** (1994) 6734, doi:10.1103/PhysRevD.50.6734, arXiv:hep-ph/9406315.
- [7] V. Kartvelishvili, R. Kvavadze, and R. Shanidze, “On Z and Z + jet production in heavy ion collisions”, *Phys. Lett. B* **356** (1995) 589, doi:10.1016/0370-2693(95)00865-I, arXiv:hep-ph/9505418.
- [8] R. Vogt, “Shadowing effects on vector boson production”, *Phys. Rev. C* **64** (2001) 044901, doi:10.1103/PhysRevC.64.044901, arXiv:hep-ph/0011242.
- [9] X.-f. Zhang and G. I. Fai, “ Z^0 production as a test of nuclear effects at the LHC”, *Phys. Lett. B* **545** (2002) 91, doi:10.1016/S0370-2693(02)02558-3, arXiv:hep-ph/0205155.
- [10] H. Paukkunen and C. A. Salgado, “Constraints for the nuclear parton distributions from Z and W production at the LHC”, *JHEP* **03** (2011) 071, doi:10.1007/JHEP03(2011)071, arXiv:1010.5392.
- [11] European Muon Collaboration, “The ratio of the nucleon structure functions F_2^N for iron and deuterium”, *Phys. Lett. B* **123** (1983) 275, doi:10.1016/0370-2693(83)90437-9.
- [12] D. de Florian, R. Sassot, P. Zurita, and M. Stratmann, “Global analysis of nuclear parton distributions”, *Phys. Rev. D* **85** (2012) 074028, doi:10.1103/PhysRevD.85.074028, arXiv:1112.6324.
- [13] H. Khanpour and S. Atashbar Tehrani, “Global analysis of nuclear parton distribution functions and their uncertainties at next-to-next-to-leading order”, *Phys. Rev. D* **93** (2016) 014026, doi:10.1103/PhysRevD.93.014026, arXiv:1601.00939.
- [14] K. J. Eskola, P. Paakkinen, H. Paukkunen, and C. A. Salgado, “EPPS16: nuclear parton distributions with LHC data”, *Eur. Phys. J. C* **77** (2017) 163, doi:10.1140/epjc/s10052-017-4725-9, arXiv:1612.05741.
- [15] K. Kovařík et al., “nCTEQ15 - Global analysis of nuclear parton distributions with uncertainties in the CTEQ framework”, *Phys. Rev. D* **93** (2016) 085037, doi:10.1103/PhysRevD.93.085037, arXiv:1509.00792.
- [16] M. Walt, I. Helenius, and W. Vogelsang, “Open-source QCD analysis of nuclear parton distribution functions at NLO and NNLO”, *Phys. Rev. D* **100** (2019) 096015, doi:10.1103/PhysRevD.100.096015, arXiv:1908.03355.

- [17] NNPDF Collaboration, “Nuclear parton distributions from lepton-nucleus scattering and the impact of an electron-ion collider”, *Eur. Phys. J. C* **79** (2019) 471, doi:[10.1140/epjc/s10052-019-6983-1](https://doi.org/10.1140/epjc/s10052-019-6983-1), arXiv:[1904.00018](https://arxiv.org/abs/1904.00018).
- [18] R. Abdul Khalek, J. J. Ethier, J. Rojo, and G. van Weelden, “nNNPDF2.0: quark flavor separation in nuclei from LHC data”, *JHEP* **09** (2020) 183, doi:[10.1007/JHEP09\(2020\)183](https://doi.org/10.1007/JHEP09(2020)183), arXiv:[2006.14629](https://arxiv.org/abs/2006.14629).
- [19] A. Kusina et al., “Impact of LHC vector boson production in heavy ion collisions on strange PDFs”, *Eur. Phys. J. C* **80** (2020) 968, doi:[10.1140/epjc/s10052-020-08532-4](https://doi.org/10.1140/epjc/s10052-020-08532-4), arXiv:[2007.09100](https://arxiv.org/abs/2007.09100).
- [20] N. Armesto, “Nuclear shadowing”, *J. Phys. G* **32** (2006) R367, doi:[10.1088/0954-3899/32/11/R01](https://doi.org/10.1088/0954-3899/32/11/R01), arXiv:[hep-ph/0604108](https://arxiv.org/abs/hep-ph/0604108).
- [21] ATLAS Collaboration, “Measurement of the high-mass Drell–Yan differential cross-section in pp collisions at $\sqrt{s} = 7$ TeV with the ATLAS detector”, *Phys. Lett. B* **725** (2013) 223, doi:[10.1016/j.physletb.2013.07.049](https://doi.org/10.1016/j.physletb.2013.07.049), arXiv:[1305.4192](https://arxiv.org/abs/1305.4192).
- [22] ATLAS Collaboration, “Measurement of the low-mass Drell–Yan differential cross section at $\sqrt{s} = 7$ TeV using the ATLAS detector”, *JHEP* **06** (2014) 112, doi:[10.1007/JHEP06\(2014\)112](https://doi.org/10.1007/JHEP06(2014)112), arXiv:[1404.1212](https://arxiv.org/abs/1404.1212).
- [23] ATLAS Collaboration, “Measurement of the double-differential high-mass Drell–Yan cross section in pp collisions at $\sqrt{s} = 8$ TeV with the ATLAS detector”, *JHEP* **08** (2016) 009, doi:[10.1007/JHEP08\(2016\)009](https://doi.org/10.1007/JHEP08(2016)009), arXiv:[1606.01736](https://arxiv.org/abs/1606.01736).
- [24] ATLAS Collaboration, “Measurement of W^\pm -boson and Z-boson production cross-sections in pp collisions at $\sqrt{s} = 2.76$ TeV with the ATLAS detector”, *Eur. Phys. J. C* **79** (2019) 901, doi:[10.1140/epjc/s10052-019-7399-7](https://doi.org/10.1140/epjc/s10052-019-7399-7), arXiv:[1907.03567](https://arxiv.org/abs/1907.03567).
- [25] ATLAS Collaboration, “Measurement of the transverse momentum distribution of Drell–Yan lepton pairs in proton–proton collisions at $\sqrt{s} = 13$ TeV with the ATLAS detector”, *Eur. Phys. J. C* **80** (2020) 616, doi:[10.1140/epjc/s10052-020-8001-z](https://doi.org/10.1140/epjc/s10052-020-8001-z), arXiv:[1912.02844](https://arxiv.org/abs/1912.02844).
- [26] CMS Collaboration, “Measurement of the Drell–Yan cross section in pp collisions at $\sqrt{s} = 7$ TeV”, *JHEP* **10** (2011) 007, doi:[10.1007/JHEP10\(2011\)007](https://doi.org/10.1007/JHEP10(2011)007), arXiv:[1108.0566](https://arxiv.org/abs/1108.0566).
- [27] CMS Collaboration, “Measurement of the differential and double-differential Drell–Yan cross sections in proton–proton collisions at $\sqrt{s} = 7$ TeV”, *JHEP* **12** (2013) 030, doi:[10.1007/JHEP12\(2013\)030](https://doi.org/10.1007/JHEP12(2013)030), arXiv:[1310.7291](https://arxiv.org/abs/1310.7291).
- [28] CMS Collaboration, “Measurements of differential and double-differential Drell–Yan cross sections in proton–proton collisions at 8 TeV”, *Eur. Phys. J. C* **75** (2015) 147, doi:[10.1140/epjc/s10052-015-3364-2](https://doi.org/10.1140/epjc/s10052-015-3364-2), arXiv:[1412.1115](https://arxiv.org/abs/1412.1115).
- [29] CMS Collaboration, “Measurement of the differential Drell–Yan cross section in proton–proton collisions at $\sqrt{s} = 13$ TeV”, *JHEP* **12** (2019) 059, doi:[10.1007/JHEP12\(2019\)059](https://doi.org/10.1007/JHEP12(2019)059), arXiv:[1812.10529](https://arxiv.org/abs/1812.10529).
- [30] CMS Collaboration, “Measurements of differential Z boson production cross sections in proton–proton collisions at $\sqrt{s} = 13$ TeV”, *JHEP* **12** (2019) 061, doi:[10.1007/JHEP12\(2019\)061](https://doi.org/10.1007/JHEP12(2019)061), arXiv:[1909.04133](https://arxiv.org/abs/1909.04133).

- [31] PHENIX Collaboration, “Measurements of $\mu\mu$ pairs from open heavy flavor and Drell–Yan in $p + p$ collisions at $\sqrt{s} = 200$ GeV”, *Phys. Rev. D* **99** (2019) 072003, doi:10.1103/PhysRevD.99.072003, arXiv:1805.02448.
- [32] ALICE Collaboration, “W and Z boson production in p-Pb collisions at $\sqrt{s_{NN}} = 5.02$ TeV”, *JHEP* **02** (2017) 077, doi:10.1007/JHEP02(2017)077, arXiv:1611.03002.
- [33] ALICE Collaboration, “Z-boson production in p-Pb collisions at $\sqrt{s_{NN}} = 8.16$ TeV and Pb-Pb collisions at $\sqrt{s_{NN}} = 5.02$ TeV”, *JHEP* **09** (2020) 076, doi:10.1007/JHEP09(2020)076, arXiv:2005.11126.
- [34] ATLAS Collaboration, “Z boson production in $p+Pb$ collisions at $\sqrt{s_{NN}} = 5.02$ TeV measured with the ATLAS detector”, *Phys. Rev. C* **92** (2015) 044915, doi:10.1103/PhysRevC.92.044915, arXiv:1507.06232.
- [35] CMS Collaboration, “Study of Z boson production in pPb collisions at $\sqrt{s_{NN}} = 5.02$ TeV”, *Phys. Lett. B* **759** (2016) 36, doi:10.1016/j.physletb.2016.05.044, arXiv:1512.06461.
- [36] A. Banfi et al., “Optimisation of variables for studying dilepton transverse momentum distributions at hadron colliders”, *Eur. Phys. J. C* **71** (2011) 1600, doi:10.1140/epjc/s10052-011-1600-y, arXiv:1009.1580.
- [37] A. Banfi, M. Dasgupta, S. Marzani, and L. Tomlinson, “Predictions for Drell–Yan ϕ^* and Q_T observables at the LHC”, *Phys. Lett. B* **715** (2012) 152, doi:10.1016/j.physletb.2012.07.035, arXiv:1205.4760.
- [38] S. Marzani, “ Q_T and ϕ^* observables in Drell–Yan processes”, *Eur. Phys. J. Web Conf.* **49** (2013) 14007, doi:10.1051/epjconf/20134914007.
- [39] CMS Collaboration, “CMS luminosity measurement using 2016 proton-nucleus collisions at nucleon-nucleon center-of-mass energy of 8.16 TeV”, CMS Physics Analysis Summary CMS-PAS-LUM-17-002, 2018.
- [40] CMS Collaboration, “The CMS experiment at the CERN LHC”, *JINST* **3** (2008) S08004, doi:10.1088/1748-0221/3/08/S08004.
- [41] CMS Collaboration, “Performance of the CMS Level-1 trigger in proton-proton collisions at $\sqrt{s} = 13$ TeV”, *JINST* **15** (2020) P10017, doi:10.1088/1748-0221/15/10/P10017, arXiv:2006.10165.
- [42] CMS Collaboration, “The CMS trigger system”, *JINST* **12** (2017) P01020, doi:10.1088/1748-0221/12/01/P01020, arXiv:1609.02366.
- [43] M. Cacciari, G. P. Salam, and G. Soyez, “The anti- k_T jet clustering algorithm”, *JHEP* **04** (2008) 063, doi:10.1088/1126-6708/2008/04/063, arXiv:0802.1189.
- [44] M. Cacciari, G. P. Salam, and G. Soyez, “FastJet user manual”, *Eur. Phys. J. C* **72** (2012) 1896, doi:10.1140/epjc/s10052-012-1896-2, arXiv:1111.6097.
- [45] CMS Collaboration, “Particle-flow reconstruction and global event description with the CMS detector”, *JINST* **12** (2017) P10003, doi:10.1088/1748-0221/12/10/P10003, arXiv:1706.04965.

- [46] CMS Collaboration, “Performance of the CMS muon detector and muon reconstruction with proton-proton collisions at $\sqrt{s} = 13$ TeV”, *JINST* **13** (2018) P06015, doi:10.1088/1748-0221/13/06/P06015, arXiv:1804.04528.
- [47] P. Nason, “A new method for combining NLO QCD with shower Monte Carlo algorithms”, *JHEP* **11** (2004) 040, doi:10.1088/1126-6708/2004/11/040, arXiv:hep-ph/0409146.
- [48] S. Frixione, P. Nason, and C. Oleari, “Matching NLO QCD computations with parton shower simulations: the POWHEG method”, *JHEP* **11** (2007) 070, doi:10.1088/1126-6708/2007/11/070, arXiv:0709.2092.
- [49] S. Alioli, P. Nason, C. Oleari, and E. Re, “A general framework for implementing NLO calculations in shower Monte Carlo programs: the POWHEG BOX”, *JHEP* **06** (2010) 043, doi:10.1007/JHEP06(2010)043, arXiv:1002.2581.
- [50] S. Alioli, P. Nason, C. Oleari, and E. Re, “NLO vector-boson production matched with shower in POWHEG”, *JHEP* **07** (2008) 060, doi:10.1088/1126-6708/2008/07/060, arXiv:0805.4802.
- [51] S. Dulat et al., “New parton distribution functions from a global analysis of quantum chromodynamics”, *Phys. Rev. D* **93** (2016) 033006, doi:10.1103/PhysRevD.93.033006, arXiv:1506.07443.
- [52] T. Sjöstrand et al., “An introduction to PYTHIA 8.2”, *Comput. Phys. Commun.* **191** (2015) 159, doi:10.1016/j.cpc.2015.01.024, arXiv:1410.3012.
- [53] CMS Collaboration, “Event generator tunes obtained from underlying event and multiparton scattering measurements”, *Eur. Phys. J. C* **76** (2016) 155, doi:10.1140/epjc/s10052-016-3988-x, arXiv:1512.00815.
- [54] S. Jadach, J. H. Kühn, and Z. Wąs, “TAUOLA—a library of Monte Carlo programs to simulate decays of polarized τ leptons”, *Comput. Phys. Commun.* **64** (1990) 275, doi:10.1016/0010-4655(91)90038-M.
- [55] P. Gonolka and Z. Wąs, “PHOTOS Monte Carlo: a precision tool for QED corrections in Z and W decays”, *Eur. Phys. J. C* **45** (2006) 97, doi:10.1140/epjc/s2005-02396-4, arXiv:hep-ph/0506026.
- [56] T. Pierog et al., “EPOS LHC: test of collective hadronization with data measured at the CERN Large Hadron Collider”, *Phys. Rev. C* **92** (2015) 034906, doi:10.1103/PhysRevC.92.034906, arXiv:1306.0121.
- [57] CMS Collaboration, “Pseudorapidity distributions of charged hadrons in proton-lead collisions at $\sqrt{s_{\text{NN}}} = 5.02$ and 8.16 TeV”, *JHEP* **01** (2018) 045, doi:10.1007/JHEP01(2018)045, arXiv:1710.09355.
- [58] CMS Collaboration, “Centrality and pseudorapidity dependence of the transverse energy density in pPb collisions at $\sqrt{s_{\text{NN}}} = 5.02$ TeV”, *Phys. Rev. C* **100** (2019) 024902, doi:10.1103/PhysRevC.100.024902, arXiv:1810.05745.
- [59] GEANT4 Collaboration, “GEANT4—a simulation toolkit”, *Nucl. Instrum. Meth. A* **506** (2003) 250, doi:10.1016/S0168-9002(03)01368-8.

- [60] CMS Collaboration, “Measurement of the W^+W^- cross section in pp collisions at $\sqrt{s} = 8$ TeV and limits on anomalous gauge couplings”, *Eur. Phys. J. C* **76** (2016) 401, doi:10.1140/epjc/s10052-016-4219-1, arXiv:1507.03268.
- [61] CMS Collaboration, “Measurement of the WZ production cross section in pp collisions at $\sqrt{s} = 7$ and 8 TeV and search for anomalous triple gauge couplings at $\sqrt{s} = 8$ TeV”, *Eur. Phys. J. C* **77** (2017) 236, doi:10.1140/epjc/s10052-017-4730-z, arXiv:1609.05721.
- [62] CMS Collaboration, “Measurement of the $pp \rightarrow ZZ$ production cross section and constraints on anomalous triple gauge couplings in four-lepton final states at $\sqrt{s} = 8$ TeV”, *Phys. Lett. B* **740** (2015) 250, doi:10.1016/j.physletb.2014.11.059, arXiv:1406.0113. [Erratum: doi:10.1016/j.physletb.2016.04.010].
- [63] CMS Collaboration, “Observation of top quark production in proton-nucleus collisions”, *Phys. Rev. Lett.* **119** (2017) 242001, doi:10.1103/PhysRevLett.119.242001, arXiv:1709.07411.
- [64] CMS Collaboration, “Observation of nuclear modifications in W^\pm boson production in pPb collisions at $\sqrt{s_{NN}} = 8.16$ TeV”, *Phys. Lett. B* **800** (2020) 135048, doi:10.1016/j.physletb.2019.135048, arXiv:1905.01486.
- [65] D. Bourilkov, “Exploring the LHC landscape with dileptons”, (2016). arXiv:1609.08994.
- [66] CMS Collaboration, “Performance of photon reconstruction and identification with the CMS detector in proton-proton collisions at $\sqrt{s} = 8$ TeV”, *JINST* **10** (2015) P08010, doi:10.1088/1748-0221/10/08/P08010, arXiv:1502.02702.
- [67] A. Bodek et al., “Extracting muon momentum scale corrections for hadron collider experiments”, *Eur. Phys. J. C* **72** (2012) 2194, doi:10.1140/epjc/s10052-012-2194-8, arXiv:1208.3710.
- [68] G. D. Cowan, “Statistical data analysis”. Oxford Univ. Press, Oxford, 1998.
- [69] CMS Collaboration, “Measurements of inclusive W and Z cross sections in pp collisions at $\sqrt{s} = 7$ TeV”, *JHEP* **01** (2011) 080, doi:10.1007/JHEP01(2011)080, arXiv:1012.2466.
- [70] J. Butterworth et al., “PDF4LHC recommendations for LHC Run II”, *J. Phys. G* **43** (2016) 023001, doi:10.1088/0954-3899/43/2/023001, arXiv:1510.03865.
- [71] A. Buckley et al., “LHAPDF6: parton density access in the LHC precision era”, *Eur. Phys. J. C* **75** (2015) 132, doi:10.1140/epjc/s10052-015-3318-8, arXiv:1412.7420.
- [72] I. P. Lokhtin and A. M. Snigirev, “A model of jet quenching in ultrarelativistic heavy ion collisions and high- p_T hadron spectra at RHIC”, *Eur. Phys. J. C* **45** (2006) 211, doi:10.1140/epjc/s2005-02426-3, arXiv:hep-ph/0506189.
- [73] H.-L. Lai et al., “New parton distributions for collider physics”, *Phys. Rev. D* **82** (2010) 074024, doi:10.1103/PhysRevD.82.074024, arXiv:1007.2241.
- [74] F. Arleo and S. Peigné, “Disentangling shadowing from coherent energy loss using the Drell-Yan process”, *Phys. Rev. D* **95** (2017) 011502, doi:10.1103/PhysRevD.95.011502, arXiv:1512.01794.

A The CMS Collaboration

Yerevan Physics Institute, Yerevan, Armenia

A.M. Sirunyan[†], A. Tumasyan

Institut für Hochenergiephysik, Wien, Austria

W. Adam, F. Ambrogi, T. Bergauer, M. Dragicevic, J. Erö, A. Escalante Del Valle, R. Frühwirth¹, M. Jeitler¹, N. Krammer, L. Lechner, D. Liko, T. Madlener, I. Mikulec, F.M. Pitters, N. Rad, J. Schieck¹, R. Schöfbeck, M. Spanring, S. Templ, W. Waltenberger, C.-E. Wulz¹, M. Zarucki

Institute for Nuclear Problems, Minsk, Belarus

V. Chekhovsky, A. Litomin, V. Makarenko, J. Suarez Gonzalez

Universiteit Antwerpen, Antwerpen, Belgium

M.R. Darwish², E.A. De Wolf, D. Di Croce, X. Janssen, T. Kello³, A. Lelek, M. Pieters, H. Rejeb Sfar, H. Van Haevermaet, P. Van Mechelen, S. Van Putte, N. Van Remortel

Vrije Universiteit Brussel, Brussel, Belgium

F. Blekman, E.S. Bols, S.S. Chhibra, J. D'Hondt, J. De Clercq, D. Lontkovskyi, S. Lowette, I. Marchesini, S. Moortgat, A. Morton, Q. Python, S. Tavernier, W. Van Doninck, P. Van Mulders

Université Libre de Bruxelles, Bruxelles, Belgium

D. Beghin, B. Bilin, B. Clerbaux, G. De Lentdecker, B. Dorney, L. Favart, A. Grebenyuk, A.K. Kalsi, I. Makarenko, L. Moureaux, L. Pétré, A. Popov, N. Postiau, E. Starling, L. Thomas, C. Vander Velde, P. Vanlaer, D. Vannerom, L. Wezenbeek

Ghent University, Ghent, Belgium

T. Cornelis, D. Dobur, M. Gruchala, I. Khvastunov⁴, M. Niedziela, C. Roskas, K. Skovpen, M. Tytgat, W. Verbeke, B. Vermassen, M. Vit

Université Catholique de Louvain, Louvain-la-Neuve, Belgium

G. Bruno, F. Bury, C. Caputo, P. David, C. Delaere, M. Delcourt, I.S. Donertas, A. Giammanco, V. Lemaitre, K. Mondal, J. Prisciandaro, A. Taliercio, M. Teklishyn, P. Vischia, S. Wuyckens, J. Zobec

Centro Brasileiro de Pesquisas Fisicas, Rio de Janeiro, Brazil

G.A. Alves, G. Correia Silva, C. Hensel, A. Moraes

Universidade do Estado do Rio de Janeiro, Rio de Janeiro, Brazil

W.L. Aldá Júnior, E. Belchior Batista Das Chagas, H. BRANDAO MALBOUSSON, W. Carvalho, J. Chinellato⁵, E. Coelho, E.M. Da Costa, G.G. Da Silveira⁶, D. De Jesus Damiao, S. Fonseca De Souza, J. Martins⁷, D. Matos Figueiredo, M. Medina Jaime⁸, M. Melo De Almeida, C. Mora Herrera, L. Mundim, H. Nogima, P. Rebello Teles, L.J. Sanchez Rosas, A. Santoro, S.M. Silva Do Amaral, A. Sznajder, M. Thiel, E.J. Tonelli Manganote⁵, F. Torres Da Silva De Araujo, A. Vilela Pereira

Universidade Estadual Paulista ^a, Universidade Federal do ABC ^b, São Paulo, Brazil

C.A. Bernardes^a, L. Calligaris^a, T.R. Fernandez Perez Tomei^a, E.M. Gregores^b, D.S. Lemos^a, P.G. Mercadante^b, S.F. Novaes^a, Sandra S. Padula^a

Institute for Nuclear Research and Nuclear Energy, Bulgarian Academy of Sciences, Sofia, Bulgaria

A. Aleksandrov, G. Antchev, I. Atanasov, R. Hadjiiska, P. Iaydjiev, M. Misheva, M. Rodozov, M. Shopova, G. Sultanov

University of Sofia, Sofia, Bulgaria

M. Bonchev, A. Dimitrov, T. Ivanov, L. Litov, B. Pavlov, P. Petkov, A. Petrov

Beihang University, Beijing, China

W. Fang³, Q. Guo, H. Wang, L. Yuan

Department of Physics, Tsinghua University, Beijing, China

M. Ahmad, Z. Hu, Y. Wang

Institute of High Energy Physics, Beijing, China

E. Chapon, G.M. Chen⁹, H.S. Chen⁹, M. Chen, D. Leggat, H. Liao, Z. Liu, R. Sharma, A. Spiezia, J. Tao, J. Thomas-wilsker, J. Wang, H. Zhang, S. Zhang⁹, J. Zhao

State Key Laboratory of Nuclear Physics and Technology, Peking University, Beijing, China

A. Agapitos, Y. Ban, C. Chen, A. Levin, Q. Li, M. Lu, X. Lyu, Y. Mao, S.J. Qian, D. Wang, Q. Wang, J. Xiao

Sun Yat-Sen University, Guangzhou, China

Z. You

Institute of Modern Physics and Key Laboratory of Nuclear Physics and Ion-beam Application (MOE) - Fudan University, Shanghai, China

X. Gao³

Zhejiang University, Hangzhou, China

M. Xiao

Universidad de Los Andes, Bogota, Colombia

C. Avila, A. Cabrera, C. Florez, J. Fraga, A. Sarkar, M.A. Segura Delgado

Universidad de Antioquia, Medellin, Colombia

J. Jaramillo, J. Mejia Guisao, F. Ramirez, J.D. Ruiz Alvarez, C.A. Salazar González, N. Vanegas Arbelaez

University of Split, Faculty of Electrical Engineering, Mechanical Engineering and Naval Architecture, Split, Croatia

D. Giljanovic, N. Godinovic, D. Lelas, I. Puljak, T. Sculac

University of Split, Faculty of Science, Split, Croatia

Z. Antunovic, M. Kovac

Institute Rudjer Boskovic, Zagreb, Croatia

V. Brigljevic, D. Ferencek, D. Majumder, M. Roguljic, A. Starodumov¹⁰, T. Susa

University of Cyprus, Nicosia, Cyprus

M.W. Ather, A. Attikis, E. Erodotou, A. Ioannou, G. Kole, M. Kolosova, S. Konstantinou, G. Mavromanolakis, J. Mousa, C. Nicolaou, F. Ptochos, P.A. Razis, H. Rykaczewski, H. Saka, D. Tsiakkouri

Charles University, Prague, Czech Republic

M. Finger¹¹, M. Finger Jr.¹¹, A. Kveton, J. Tomsa

Escuela Politecnica Nacional, Quito, Ecuador

E. Ayala

Universidad San Francisco de Quito, Quito, Ecuador

E. Carrera Jarrin

Academy of Scientific Research and Technology of the Arab Republic of Egypt, Egyptian Network of High Energy Physics, Cairo, Egypt
 S. Abu Zeid¹², Y. Assran^{13,14}, A. Ellithi Kamel¹⁵

Center for High Energy Physics (CHEP-FU), Fayoum University, El-Fayoum, Egypt
 A. Lotfy, M.A. Mahmoud

National Institute of Chemical Physics and Biophysics, Tallinn, Estonia
 S. Bhowmik, A. Carvalho Antunes De Oliveira, R.K. Dewanjee, K. Ehataht, M. Kadastik, M. Raidal, C. Veelken

Department of Physics, University of Helsinki, Helsinki, Finland
 P. Eerola, L. Forthomme, H. Kirschenmann, K. Osterberg, M. Voutilainen

Helsinki Institute of Physics, Helsinki, Finland
 E. Brücken, F. Garcia, J. Havukainen, V. Karimäki, M.S. Kim, R. Kinnunen, T. Lampén, K. Lassila-Perini, S. Laurila, S. Lehti, T. Lindén, H. Siikonen, E. Tuominen, J. Tuominiemi

Lappeenranta University of Technology, Lappeenranta, Finland
 P. Luukka, T. Tuuva

IRFU, CEA, Université Paris-Saclay, Gif-sur-Yvette, France
 C. Amendola, M. Besancon, F. Couderc, M. Dejardin, D. Denegri, J.L. Faure, F. Ferri, S. Ganjour, A. Givernaud, P. Gras, G. Hamel de Monchenault, P. Jarry, B. Lenzi, E. Locci, J. Malcles, J. Rander, A. Rosowsky, M.Ö. Sahin, A. Savoy-Navarro¹⁶, M. Titov, G.B. Yu

Laboratoire Leprince-Ringuet, CNRS/IN2P3, Ecole Polytechnique, Institut Polytechnique de Paris, Palaiseau, France
 S. Ahuja, F. Beaudette, M. Bonanomi, A. Buchot Perraguin, P. Busson, C. Charlot, O. Davignon, B. Diab, G. Falmagne, R. Granier de Cassagnac, A. Hakimi, I. Kucher, A. Lobanov, C. Martin Perez, M. Nguyen, C. Ochando, P. Paganini, J. Rembser, R. Salerno, J.B. Sauvan, Y. Sirois, A. Zabi, A. Zghiche

Université de Strasbourg, CNRS, IPHC UMR 7178, Strasbourg, France
 J.-L. Agram¹⁷, J. Andrea, D. Bloch, G. Bourgatte, J.-M. Brom, E.C. Chabert, C. Collard, J.-C. Fontaine¹⁷, D. Gelé, U. Goerlach, C. Grimault, A.-C. Le Bihan, P. Van Hove

Institut de Physique des 2 Infinis de Lyon (IP2I), Villeurbanne, France
 E. Asilar, S. Beauceron, C. Bernet, G. Boudoul, C. Camen, A. Carle, N. Chanon, D. Contardo, P. Depasse, H. El Mamouni, J. Fay, S. Gascon, M. Gouzevitch, B. Ille, Sa. Jain, I.B. Laktineh, H. Lattauad, A. Lesauvage, M. Lethuillier, L. Mirabito, L. Torterotot, G. Touquet, M. Vander Donckt, S. Viret

Georgian Technical University, Tbilisi, Georgia
 T. Toriashvili¹⁸, Z. Tsamalaidze¹¹

RWTH Aachen University, I. Physikalisches Institut, Aachen, Germany
 L. Feld, K. Klein, M. Lipinski, D. Meuser, A. Pauls, M. Preuten, M.P. Rauch, J. Schulz, M. Teroerde

RWTH Aachen University, III. Physikalisches Institut A, Aachen, Germany
 D. Eliseev, M. Erdmann, P. Fackeldey, B. Fischer, S. Ghosh, T. Hebbeker, K. Hoepfner, H. Keller, L. Mastrolorenzo, M. Merschmeyer, A. Meyer, P. Millet, G. Mocellin, S. Mondal, S. Mukherjee, D. Noll, A. Novak, T. Pook, A. Pozdnyakov, T. Quast, M. Radziej, Y. Rath, H. Reithler, J. Roemer, A. Schmidt, S.C. Schuler, A. Sharma, S. Wiedenbeck, S. Zaleski

RWTH Aachen University, III. Physikalisches Institut B, Aachen, Germany

C. Dziwok, G. Flügge, W. Haj Ahmad¹⁹, O. Hlushchenko, T. Kress, A. Nowack, C. Pistone, O. Pooth, D. Roy, H. Sert, A. Stahl²⁰, T. Ziemons

Deutsches Elektronen-Synchrotron, Hamburg, Germany

H. Aarup Petersen, M. Aldaya Martin, P. Asmuss, I. Babounikau, S. Baxter, O. Behnke, A. Bermúdez Martínez, A.A. Bin Anuar, K. Borras²¹, V. Botta, D. Brunner, A. Campbell, A. Cardini, P. Connor, S. Consuegra Rodríguez, V. Danilov, A. De Wit, M.M. Defranchis, L. Didukh, D. Domínguez Damiani, G. Eckerlin, D. Eckstein, T. Eichhorn, L.I. Estevez Banos, E. Gallo²², A. Geiser, A. Giraldi, A. Grohsjean, M. Guthoff, A. Harb, A. Jafari²³, N.Z. Jomhari, H. Jung, A. Kasem²¹, M. Kasemann, H. Kaveh, C. Kleinwort, J. Knolle, D. Krücker, W. Lange, T. Lenz, J. Lidrych, K. Lipka, W. Lohmann²⁴, R. Mankel, I.-A. Melzer-Pellmann, J. Metwally, A.B. Meyer, M. Meyer, M. Missiroli, J. Mnich, A. Mussgiller, V. Myronenko, Y. Otarid, D. Pérez Adán, S.K. Pflitsch, D. Pitzl, A. Raspereza, A. Saggio, A. Saibel, M. Savitskyi, V. Scheurer, P. Schütze, C. Schwanenberger, A. Singh, R.E. Sosa Ricardo, N. Tonon, O. Turkot, A. Vagnerini, M. Van De Klundert, R. Walsh, D. Walter, Y. Wen, K. Wichmann, C. Wissing, S. Wuchterl, O. Zenaiev, R. Zlebcik

University of Hamburg, Hamburg, Germany

R. Aggleton, S. Bein, L. Benato, A. Benecke, K. De Leo, T. Dreyer, A. Ebrahimi, M. Eich, F. Feindt, A. Fröhlich, C. Garbers, E. Garutti, P. Gunnellini, J. Haller, A. Hinzmann, A. Karavdina, G. Kasieczka, R. Klanner, R. Kogler, V. Kutzner, J. Lange, T. Lange, A. Malara, C.E.N. Niemeyer, A. Nigamova, K.J. Pena Rodriguez, O. Rieger, P. Schleper, S. Schumann, J. Schwandt, D. Schwarz, J. Sonneveld, H. Stadie, G. Steinbrück, B. Vormwald, I. Zoi

Karlsruher Institut fuer Technologie, Karlsruhe, Germany

M. Baselga, S. Baur, J. Bechtel, T. Berger, E. Butz, R. Caspart, T. Chwalek, W. De Boer, A. Dierlamm, A. Droll, K. El Morabit, N. Faltermann, K. Flöh, M. Giffels, A. Gottmann, F. Hartmann²⁰, C. Heidecker, U. Husemann, M.A. Iqbal, I. Katkov²⁵, P. Keicher, R. Koppenhöfer, S. Maier, M. Metzler, S. Mitra, D. Müller, Th. Müller, M. Musich, G. Quast, K. Rabbertz, J. Rauser, D. Savoiu, D. Schäfer, M. Schnepf, M. Schröder, D. Seith, I. Shvetsov, H.J. Simonis, R. Ulrich, M. Wassmer, M. Weber, R. Wolf, S. Wozniewski

Institute of Nuclear and Particle Physics (INPP), NCSR Demokritos, Aghia Paraskevi, Greece

G. Anagnostou, P. Asenov, G. Daskalakis, T. Geralis, A. Kyriakis, D. Loukas, G. Paspalaki, A. Stakia

National and Kapodistrian University of Athens, Athens, Greece

M. Diamantopoulou, D. Karasavvas, G. Karathanasis, P. Kontaxakis, C.K. Koraka, A. Manousakis-katsikakis, A. Panagiotou, I. Papavergou, N. Saoulidou, K. Theofilatos, K. Vellidis, E. Vourliotis

National Technical University of Athens, Athens, Greece

G. Bakas, K. Kousouris, I. Papakrivopoulos, G. Tsipolitis, A. Zacharopoulou

University of Ioánnina, Ioánnina, Greece

I. Evangelou, C. Foudas, P. Gianneios, P. Katsoulis, P. Kokkas, S. Mallios, K. Manitara, N. Manthos, I. Papadopoulos, J. Strologas

MTA-ELTE Lendület CMS Particle and Nuclear Physics Group, Eötvös Loránd University,

Budapest, Hungary

M. Bartók²⁶, R. Chudasama, M. Csanad, M.M.A. Gadallah²⁷, S. Lökö²⁸, P. Major, K. Mandal, A. Mehta, G. Pasztor, O. Surányi, G.I. Veres

Wigner Research Centre for Physics, Budapest, Hungary

G. Bencze, C. Hajdu, D. Horvath²⁹, F. Sikler, V. Veszpremi, G. Vesztregombi[†]

Institute of Nuclear Research ATOMKI, Debrecen, Hungary

S. Czellar, J. Karancsi²⁶, J. Molnar, Z. Szillasi, D. Teyssier

Institute of Physics, University of Debrecen, Debrecen, Hungary

P. Raics, Z.L. Trocsanyi, B. Ujvari

Eszterhazy Karoly University, Karoly Robert Campus, Gyongyos, Hungary

T. Csorgo, F. Nemes, T. Novak

Indian Institute of Science (IISc), Bangalore, India

S. Choudhury, J.R. Komaragiri, D. Kumar, L. Panwar, P.C. Tiwari

National Institute of Science Education and Research, HBNI, Bhubaneswar, India

S. Bahinipati³⁰, D. Dash, C. Kar, P. Mal, T. Mishra, V.K. Muraleedharan Nair Bindhu, A. Nayak³¹, D.K. Sahoo³⁰, N. Sur, S.K. Swain

Punjab University, Chandigarh, India

S. Bansal, S.B. Beri, V. Bhatnagar, S. Chauhan, N. Dhingra³², R. Gupta, A. Kaur, S. Kaur, P. Kumari, M. Lohan, M. Meena, K. Sandeep, S. Sharma, J.B. Singh, A.K. Virdi

University of Delhi, Delhi, India

A. Ahmed, A. Bhardwaj, B.C. Choudhary, R.B. Garg, M. Gola, S. Keshri, A. Kumar, M. Naimuddin, P. Priyanka, K. Ranjan, A. Shah

Saha Institute of Nuclear Physics, HBNI, Kolkata, India

M. Bharti³³, R. Bhattacharya, S. Bhattacharya, D. Bhowmik, S. Dutta, S. Ghosh, B. Gomber³⁴, M. Maity³⁵, S. Nandan, P. Palit, A. Purohit, P.K. Rout, G. Saha, S. Sarkar, M. Sharan, B. Singh³³, S. Thakur³³

Indian Institute of Technology Madras, Madras, India

P.K. Behera, S.C. Behera, P. Kalbhor, A. Muhammad, R. Pradhan, P.R. Pujahari, A. Sharma, A.K. Sikdar

Bhabha Atomic Research Centre, Mumbai, India

D. Dutta, V. Kumar, K. Naskar³⁶, P.K. Netrakanti, L.M. Pant, P. Shukla

Tata Institute of Fundamental Research-A, Mumbai, India

T. Aziz, M.A. Bhat, S. Dugad, R. Kumar Verma, U. Sarkar

Tata Institute of Fundamental Research-B, Mumbai, India

S. Banerjee, S. Bhattacharya, S. Chatterjee, M. Guchait, S. Karmakar, S. Kumar, G. Majumder, K. Mazumdar, S. Mukherjee, D. Roy, N. Sahoo

Indian Institute of Science Education and Research (IISER), Pune, India

S. Dube, B. Kansal, A. Kapoor, K. Kothekar, S. Pandey, A. Rane, A. Rastogi, S. Sharma

Department of Physics, Isfahan University of Technology, Isfahan, Iran

H. Bakhshiansohi³⁷

Institute for Research in Fundamental Sciences (IPM), Tehran, IranS. Chenarani³⁸, S.M. Etesami, M. Khakzad, M. Mohammadi Najafabadi**University College Dublin, Dublin, Ireland**

M. Felcini, M. Grunewald

INFN Sezione di Bari ^a, Università di Bari ^b, Politecnico di Bari ^c, Bari, ItalyM. Abbrescia^{a,b}, R. Aly^{a,b,39}, C. Aruta^{a,b}, A. Colaleo^a, D. Creanza^{a,c}, N. De Filippis^{a,c}, M. De Palma^{a,b}, A. Di Florio^{a,b}, A. Di Pilato^{a,b}, W. Elmetenawee^{a,b}, L. Fiore^a, A. Gelmi^{a,b}, M. Gul^a, G. Iaselli^{a,c}, M. Ince^{a,b}, S. Lezki^{a,b}, G. Maggi^{a,c}, M. Maggi^a, I. Margjeka^{a,b}, V. Mastrapasqua^{a,b}, J.A. Merlin^a, S. My^{a,b}, S. Nuzzo^{a,b}, A. Pompili^{a,b}, G. Pugliese^{a,c}, A. Ranieri^a, G. Selvaggi^{a,b}, L. Silvestris^a, F.M. Simone^{a,b}, R. Venditti^a, P. Verwilligen^a**INFN Sezione di Bologna ^a, Università di Bologna ^b, Bologna, Italy**G. Abbiendi^a, C. Battilana^{a,b}, D. Bonacorsi^{a,b}, L. Borgonovi^{a,b}, S. Braibant-Giacomelli^{a,b}, R. Campanini^{a,b}, P. Capiluppi^{a,b}, A. Castro^{a,b}, F.R. Cavallo^a, M. Cuffiani^{a,b}, G.M. Dallavalle^a, T. Diotalevi^{a,b}, F. Fabbri^a, A. Fanfani^{a,b}, E. Fontanesi^{a,b}, P. Giacomelli^a, L. Giommi^{a,b}, C. Grandi^a, L. Guiducci^{a,b}, F. Iemmi^{a,b}, S. Lo Meo^{a,40}, S. Marcellini^a, G. Masetti^a, F.L. Navarria^{a,b}, A. Perrotta^a, F. Primavera^{a,b}, A.M. Rossi^{a,b}, T. Rovelli^{a,b}, G.P. Siroli^{a,b}, N. Tosi^a**INFN Sezione di Catania ^a, Università di Catania ^b, Catania, Italy**S. Albergo^{a,b,41}, S. Costa^{a,b,41}, A. Di Mattia^a, R. Potenza^{a,b}, A. Tricomi^{a,b,41}, C. Tuve^{a,b}**INFN Sezione di Firenze ^a, Università di Firenze ^b, Firenze, Italy**G. Barbagli^a, A. Cassese^a, R. Ceccarelli^{a,b}, V. Ciulli^{a,b}, C. Civinini^a, R. D'Alessandro^{a,b}, F. Fiori^a, E. Focardi^{a,b}, G. Latino^{a,b}, P. Lenzi^{a,b}, M. Lizzo^{a,b}, M. Meschini^a, S. Paoletti^a, R. Seidita^{a,b}, G. Sguazzoni^a, L. Viliani^a**INFN Laboratori Nazionali di Frascati, Frascati, Italy**

L. Benussi, S. Bianco, D. Piccolo

INFN Sezione di Genova ^a, Università di Genova ^b, Genova, ItalyM. Bozzo^{a,b}, F. Ferro^a, R. Mulargia^{a,b}, E. Robutti^a, S. Tosi^{a,b}**INFN Sezione di Milano-Bicocca ^a, Università di Milano-Bicocca ^b, Milano, Italy**A. Benaglia^a, A. Beschi^{a,b}, F. Brivio^{a,b}, F. Cetorelli^{a,b}, V. Ciriolo^{a,b,20}, F. De Guio^{a,b}, M.E. Dinardo^{a,b}, P. Dini^a, S. Gennai^a, A. Ghezzi^{a,b}, P. Govoni^{a,b}, L. Guzzi^{a,b}, M. Malberti^a, S. Malvezzi^a, D. Menasce^a, F. Monti^{a,b}, L. Moroni^a, M. Paganoni^{a,b}, D. Pedrini^a, S. Ragazzi^{a,b}, T. Tabarelli de Fatis^{a,b}, D. Valsecchi^{a,b,20}, D. Zuolo^{a,b}**INFN Sezione di Napoli ^a, Università di Napoli 'Federico II' ^b, Napoli, Italy, Università della Basilicata ^c, Potenza, Italy, Università G. Marconi ^d, Roma, Italy**S. Buontempo^a, N. Cavallo^{a,c}, A. De Iorio^{a,b}, F. Fabozzi^{a,c}, F. Fienga^a, A.O.M. Iorio^{a,b}, L. Layer^{a,b}, L. Lista^{a,b}, S. Meola^{a,d,20}, P. Paolucci^{a,20}, B. Rossi^a, C. Sciacca^{a,b}, E. Voevodina^{a,b}**INFN Sezione di Padova ^a, Università di Padova ^b, Padova, Italy, Università di Trento ^c, Trento, Italy**P. Azzi^a, N. Bacchetta^a, D. Bisello^{a,b}, A. Boletti^{a,b}, A. Bragagnolo^{a,b}, R. Carlin^{a,b}, P. Checchia^a, P. De Castro Manzano^a, T. Dorigo^a, F. Gasparini^{a,b}, U. Gasparini^{a,b}, S.Y. Hoh^{a,b}, M. Margoni^{a,b}, A.T. Meneguzzo^{a,b}, M. Presilla^b, P. Ronchese^{a,b}, R. Rossin^{a,b}, F. Simonetto^{a,b}, G. Strong, A. Tiko^a, M. Tosi^{a,b}, M. Zanetti^{a,b}, P. Zotto^{a,b}, A. Zucchetta^{a,b}, G. Zumerle^{a,b}**INFN Sezione di Pavia ^a, Università di Pavia ^b, Pavia, Italy**C. Aime^{a,b}, A. Braghieri^a, S. Calzaferri^{a,b}, D. Fiorina^{a,b}, P. Montagna^{a,b}, S.P. Ratti^{a,b}, V. Re^a, M. Ressegotti^{a,b}, C. Riccardi^{a,b}, P. Salvini^a, I. Vai^a, P. Vitulo^{a,b}

INFN Sezione di Perugia ^a, Università di Perugia ^b, Perugia, Italy

M. Biasini^{a,b}, G.M. Bilei^a, D. Ciangottini^{a,b}, L. Fanò^{a,b}, P. Lariccia^{a,b}, G. Mantovani^{a,b}, V. Mariani^{a,b}, M. Menichelli^a, F. Moscatelli^a, A. Rossi^{a,b}, A. Santocchia^{a,b}, D. Spiga^a, T. Tedeschia^{a,b}

INFN Sezione di Pisa ^a, Università di Pisa ^b, Scuola Normale Superiore di Pisa ^c, Pisa Italy, Università di Siena ^d, Siena, Italy

K. Androsov^a, P. Azzurri^a, G. Bagliesi^a, V. Bertacchi^{a,c}, L. Bianchini^a, T. Boccali^a, R. Castaldi^a, M.A. Ciocci^{a,b}, R. Dell'Orso^a, M.R. Di Domenico^{a,d}, S. Donato^a, L. Giannini^{a,c}, A. Giassi^a, M.T. Grippo^a, F. Ligabue^{a,c}, E. Manca^{a,c}, G. Mandorli^{a,c}, A. Messineo^{a,b}, F. Palla^a, G. Ramirez-Sanchez^{a,c}, A. Rizzi^{a,b}, G. Rolandi^{a,c}, S. Roy Chowdhury^{a,c}, A. Scribano^a, N. Shafiei^{a,b}, P. Spagnolo^a, R. Tenchini^a, G. Tonelli^{a,b}, N. Turini^{a,d}, A. Venturi^a, P.G. Verdini^a

INFN Sezione di Roma ^a, Sapienza Università di Roma ^b, Rome, Italy

F. Cavallari^a, M. Cipriani^{a,b}, D. Del Re^{a,b}, E. Di Marco^a, M. Diemoz^a, E. Longo^{a,b}, P. Meridiani^a, G. Organtini^{a,b}, F. Pandolfi^a, R. Paramatti^{a,b}, C. Quaranta^{a,b}, S. Rahatlou^{a,b}, C. Rovelli^a, F. Santanastasio^{a,b}, L. Soffi^{a,b}, R. Tramontano^{a,b}

INFN Sezione di Torino ^a, Università di Torino ^b, Torino, Italy, Università del Piemonte Orientale ^c, Novara, Italy

N. Amapane^{a,b}, R. Arcidiacono^{a,c}, S. Argiro^{a,b}, M. Arneodo^{a,c}, N. Bartosik^a, R. Bellan^{a,b}, A. Bellora^{a,b}, C. Biino^a, A. Cappati^{a,b}, N. Cartiglia^a, S. Cometti^a, M. Costa^{a,b}, R. Covarelli^{a,b}, N. Demaria^a, B. Kiani^{a,b}, F. Legger^a, C. Mariotti^a, S. Maselli^a, E. Migliore^{a,b}, V. Monaco^{a,b}, E. Monteil^{a,b}, M. Monteno^a, M.M. Obertino^{a,b}, G. Ortona^a, L. Pacher^{a,b}, N. Pastrone^a, M. Pelliccioni^a, G.L. Pinna Angionia^{a,b}, M. Ruspa^{a,c}, R. Salvatico^{a,b}, F. Siviero^{a,b}, V. Sola^a, A. Solano^{a,b}, D. Soldi^{a,b}, A. Staiano^a, D. Trocino^{a,b}

INFN Sezione di Trieste ^a, Università di Trieste ^b, Trieste, Italy

S. Belforte^a, V. Candelise^{a,b}, M. Casarsa^a, F. Cossutti^a, A. Da Rold^{a,b}, G. Della Ricca^{a,b}, F. Vazzoler^{a,b}

Kyungpook National University, Daegu, Korea

S. Dogra, C. Huh, B. Kim, D.H. Kim, G.N. Kim, J. Lee, S.W. Lee, C.S. Moon, Y.D. Oh, S.I. Pak, B.C. Radburn-Smith, S. Sekmen, Y.C. Yang

Chonnam National University, Institute for Universe and Elementary Particles, Kwangju, Korea

H. Kim, D.H. Moon

Hanyang University, Seoul, Korea

B. Francois, T.J. Kim, J. Park

Korea University, Seoul, Korea

S. Cho, S. Choi, Y. Go, S. Ha, B. Hong, K. Lee, K.S. Lee, J. Lim, J. Park, S.K. Park, J. Yoo

Kyung Hee University, Department of Physics, Seoul, Republic of Korea

J. Goh, A. Gurtu

Sejong University, Seoul, Korea

H.S. Kim, Y. Kim

Seoul National University, Seoul, Korea

J. Almond, J.H. Bhyun, J. Choi, S. Jeon, J. Kim, J.S. Kim, S. Ko, H. Kwon, H. Lee, K. Lee, S. Lee, K. Nam, B.H. Oh, M. Oh, S.B. Oh, H. Seo, U.K. Yang, I. Yoon

University of Seoul, Seoul, Korea

D. Jeon, J.H. Kim, B. Ko, J.S.H. Lee, I.C. Park, Y. Roh, D. Song, I.J. Watson

Yonsei University, Department of Physics, Seoul, Korea

H.D. Yoo

Sungkyunkwan University, Suwon, Korea

Y. Choi, C. Hwang, Y. Jeong, H. Lee, Y. Lee, I. Yu

College of Engineering and Technology, American University of the Middle East (AUM), Egaila, Kuwait

Y. Maghrbi

Riga Technical University, Riga, Latvia

V. Veckalns⁴²

Vilnius University, Vilnius, Lithuania

A. Juodagalvis, A. Rinkevicius, G. Tamulaitis

National Centre for Particle Physics, Universiti Malaya, Kuala Lumpur, Malaysia

W.A.T. Wan Abdullah, M.N. Yusli, Z. Zolkapli

Universidad de Sonora (UNISON), Hermosillo, Mexico

J.F. Benitez, A. Castaneda Hernandez, J.A. Murillo Quijada, L. Valencia Palomo

Centro de Investigacion y de Estudios Avanzados del IPN, Mexico City, Mexico

H. Castilla-Valdez, E. De La Cruz-Burelo, I. Heredia-De La Cruz⁴³, R. Lopez-Fernandez, A. Sanchez-Hernandez

Universidad Iberoamericana, Mexico City, Mexico

S. Carrillo Moreno, C. Oropeza Barrera, M. Ramirez-Garcia, F. Vazquez Valencia

Benemerita Universidad Autonoma de Puebla, Puebla, Mexico

J. Eysermans, I. Pedraza, H.A. Salazar Ibarguen, C. Uribe Estrada

Universidad Autónoma de San Luis Potosí, San Luis Potosí, Mexico

A. Morelos Pineda

University of Montenegro, Podgorica, Montenegro

J. Mijuskovic⁴, N. Raicevic

University of Auckland, Auckland, New Zealand

D. Kofcheck

University of Canterbury, Christchurch, New Zealand

S. Bheesette, P.H. Butler

National Centre for Physics, Quaid-I-Azam University, Islamabad, Pakistan

A. Ahmad, M.I. Asghar, M.I.M. Awan, H.R. Hoorani, W.A. Khan, M.A. Shah, M. Shoaib, M. Waqas

AGH University of Science and Technology Faculty of Computer Science, Electronics and Telecommunications, Krakow, Poland

V. Avati, L. Grzanka, M. Malawski

National Centre for Nuclear Research, Swierk, Poland

H. Bialkowska, M. Bluj, B. Boimska, T. Frueboes, M. Górski, M. Kazana, M. Szleper, P. Traczyk, P. Zalewski

Institute of Experimental Physics, Faculty of Physics, University of Warsaw, Warsaw, Poland
 K. Bunkowski, A. Byszuk⁴⁴, K. Doroba, A. Kalinowski, M. Konecki, J. Krolikowski,
 M. Olszewski, M. Walczak

Laboratório de Instrumentação e Física Experimental de Partículas, Lisboa, Portugal
 M. Araujo, P. Bargassa, D. Bastos, P. Faccioli, M. Gallinaro, J. Hollar, N. Leonardo, T. Niknejad,
 J. Seixas, K. Shchelina, O. Toldaiev, J. Varela

Joint Institute for Nuclear Research, Dubna, Russia

S. Afanasiev, P. Bunin, M. Gavrilko, I. Golutvin, I. Gorbunov, A. Kamenev, V. Karjavine,
 A. Lanev, A. Malakhov, V. Matveev^{45,46}, P. Moisenz, V. Palichik, V. Perelygin, M. Savina,
 S. Shmatov, S. Shulha, V. Smirnov, O. Teryaev, V. Trofimov, N. Voityshin, B.S. Yuldashev⁴⁷,
 A. Zarubin, I. Zhizhin

Petersburg Nuclear Physics Institute, Gatchina (St. Petersburg), Russia

G. Gavrilov, V. Golovtcov, Y. Ivanov, V. Kim⁴⁸, E. Kuznetsova⁴⁹, V. Murzin, V. Oreshkin,
 I. Smirnov, D. Sosnov, V. Sulimov, L. Uvarov, S. Volkov, A. Vorobyev

Institute for Nuclear Research, Moscow, Russia

Yu. Andreev, A. Dermenev, S. Gninenko, N. Golubev, A. Karneyeu, M. Kirsanov, N. Krasnikov,
 A. Pashenkov, G. Pivovarov, D. Tlisov[†], A. Toropin

**Institute for Theoretical and Experimental Physics named by A.I. Alikhanov of NRC
 'Kurchatov Institute', Moscow, Russia**

V. Epshteyn, V. Gavrilov, N. Lychkovskaya, A. Nikitenko⁵⁰, V. Popov, G. Safronov,
 A. Spiridonov, A. Stepenov, M. Toms, E. Vlasov, A. Zhokin

Moscow Institute of Physics and Technology, Moscow, Russia

T. Aushev

**National Research Nuclear University 'Moscow Engineering Physics Institute' (MEPhI),
 Moscow, Russia**

O. Bychkova, M. Chadeeva⁵¹, D. Philippov, E. Popova, V. Rusinov

P.N. Lebedev Physical Institute, Moscow, Russia

V. Andreev, M. Azarkin, I. Dremin, M. Kirakosyan, A. Terkulov

**Skobeltsyn Institute of Nuclear Physics, Lomonosov Moscow State University, Moscow,
 Russia**

A. Belyaev, E. Boos, V. Bunichev, A. Ershov, A. Gribushin, O. Kodolova, V. Korotkikh, I. Loktin,
 S. Obraztsov, S. Petrushanko, V. Savrin, A. Snigirev, I. Vardanyan

Novosibirsk State University (NSU), Novosibirsk, Russia

V. Blinov⁵², T. Dimova⁵², L. Kardapoltsev⁵², I. Ovtin⁵², Y. Skovpen⁵²

**Institute for High Energy Physics of National Research Centre 'Kurchatov Institute',
 Protvino, Russia**

I. Azhgirey, I. Bayshev, V. Kachanov, A. Kalinin, D. Konstantinov, V. Petrov, R. Ryutin, A. Sobol,
 S. Troshin, N. Tyurin, A. Uzunian, A. Volkov

National Research Tomsk Polytechnic University, Tomsk, Russia

A. Babaev, A. Iuzhakov, V. Okhotnikov, L. Sukhikh

Tomsk State University, Tomsk, Russia

V. Borchsh, V. Ivanchenko, E. Tcherniaev

University of Belgrade: Faculty of Physics and VINCA Institute of Nuclear Sciences, Belgrade, Serbia

P. Adzic⁵³, P. Cirkovic, M. Dordevic, P. Milenovic, J. Milosevic

Centro de Investigaciones Energéticas Medioambientales y Tecnológicas (CIEMAT), Madrid, Spain

M. Aguilar-Benitez, J. Alcaraz Maestre, A. Álvarez Fernández, I. Bachiller, M. Barrio Luna, Cristina F. Bedoya, J.A. Brochero Cifuentes, C.A. Carrillo Montoya, M. Cepeda, M. Cerrada, N. Colino, B. De La Cruz, A. Delgado Peris, J.P. Fernández Ramos, J. Flix, M.C. Fouz, A. García Alonso, O. Gonzalez Lopez, S. Goy Lopez, J.M. Hernandez, M.I. Josa, J. León Holgado, D. Moran, Á. Navarro Tobar, A. Pérez-Calero Yzquierdo, J. Puerta Pelayo, I. Redondo, L. Romero, S. Sánchez Navas, M.S. Soares, A. Triossi, L. Urda Gómez, C. Willmott

Universidad Autónoma de Madrid, Madrid, Spain

C. Albajar, J.F. de Trocóniz, R. Reyes-Almanza

Universidad de Oviedo, Instituto Universitario de Ciencias y Tecnologías Espaciales de Asturias (ICTEA), Oviedo, Spain

B. Alvarez Gonzalez, J. Cuevas, C. Erice, J. Fernandez Menendez, S. Folgueras, I. González Caballero, E. Palencia Cortezon, C. Ramón Álvarez, J. Ripoll Sau, V. Rodríguez Bouza, S. Sanchez Cruz, A. Trapote

Instituto de Física de Cantabria (IFCA), CSIC-Universidad de Cantabria, Santander, Spain

I.J. Cabrillo, A. Calderon, B. Chazin Quero, J. Duarte Campderros, M. Fernandez, P.J. Fernández Manteca, G. Gomez, C. Martinez Rivero, P. Martinez Ruiz del Arbol, F. Matorras, J. Piedra Gomez, C. Prieels, F. Ricci-Tam, T. Rodrigo, A. Ruiz-Jimeno, L. Scodellaro, I. Vila, J.M. Vizan Garcia

University of Colombo, Colombo, Sri Lanka

MK Jayananda, B. Kailasapathy⁵⁴, D.U.J. Sonnadara, DDC Wickramarathna

University of Ruhuna, Department of Physics, Matara, Sri Lanka

W.G.D. Dharmaratna, K. Liyanage, N. Perera, N. Wickramage

CERN, European Organization for Nuclear Research, Geneva, Switzerland

T.K. Arrestad, D. Abbaneo, B. Akgun, E. Auffray, G. Auzinger, J. Baechler, P. Baillon, A.H. Ball, D. Barney, J. Bendavid, N. Beni, M. Bianco, A. Bocci, P. Bortignon, E. Bossini, E. Brondolin, T. Camporesi, G. Cerminara, L. Cristella, D. d'Enterria, A. Dabrowski, N. Daci, V. Daponte, A. David, A. De Roeck, M. Deile, R. Di Maria, M. Dobson, M. Dünser, N. Dupont, A. Elliott-Peisert, N. Emriskova, F. Fallavollita⁵⁵, D. Fasanella, S. Fiorendi, G. Franzoni, J. Fulcher, W. Funk, S. Giani, D. Gigi, K. Gill, F. Glege, L. Gouskos, M. Guilbaud, D. Gulhan, M. Haranko, J. Hegeman, Y. Iiyama, V. Innocente, T. James, P. Janot, J. Kaspar, J. Kieseler, M. Komm, N. Kratochwil, C. Lange, P. Lecoq, K. Long, C. Lourenço, L. Malgeri, M. Mannelli, A. Massironi, F. Meijers, S. Mersi, E. Meschi, F. Moortgat, M. Mulders, J. Ngadiuba, J. Niedziela, S. Orfanelli, L. Orsini, F. Pantaleo²⁰, L. Pape, E. Perez, M. Peruzzi, A. Petrilli, G. Petrucciani, A. Pfeiffer, M. Pierini, D. Rabady, A. Racz, M. Rieger, M. Rovere, H. Sakulin, J. Salfeld-Nebgen, S. Scarfi, C. Schäfer, C. Schwick, M. Selvaggi, A. Sharma, P. Silva, W. Snoeys, P. Sphicas⁵⁶, J. Steggemann, S. Summers, V.R. Tavolaro, D. Treille, A. Tsirou, G.P. Van Onsem, A. Vartak, M. Verzetti, K.A. Wozniak, W.D. Zeuner

Paul Scherrer Institut, Villigen, Switzerland

L. Caminada⁵⁷, W. Erdmann, R. Horisberger, Q. Ingram, H.C. Kaestli, D. Kotlinski, U. Langenegger, T. Rohe

ETH Zurich - Institute for Particle Physics and Astrophysics (IPA), Zurich, Switzerland

M. Backhaus, P. Berger, A. Calandri, N. Chernyavskaya, A. De Cosa, G. Dissertori, M. Dittmar, M. Donegà, C. Dorfer, T. Gadek, T.A. Gómez Espinosa, C. Grab, D. Hits, W. Lustermann, A.-M. Lyon, R.A. Manzoni, M.T. Meinhard, F. Micheli, F. Nessi-Tedaldi, F. Pauss, V. Perovic, G. Perrin, L. Perrozzi, S. Pigazzini, M.G. Ratti, M. Reichmann, C. Reissel, T. Reitenspiess, B. Ristic, D. Ruini, D.A. Sanz Becerra, M. Schönenberger, V. Stampf, M.L. Vesterbacka Olsson, R. Wallny, D.H. Zhu

Universität Zürich, Zurich, Switzerland

C. Amsler⁵⁸, C. Botta, D. Brzhechko, M.F. Canelli, R. Del Burgo, J.K. Heikkilä, M. Huwiler, A. Jofrehei, B. Kilminster, S. Leontsinis, A. Macchiolo, P. Meiring, V.M. Mikuni, U. Molinatti, I. Neutelings, G. Rauco, A. Reimers, P. Robmann, K. Schweiger, Y. Takahashi, S. Wertz

National Central University, Chung-Li, Taiwan

C. Adloff⁵⁹, C.M. Kuo, W. Lin, A. Roy, T. Sarkar³⁵, S.S. Yu

National Taiwan University (NTU), Taipei, Taiwan

L. Ceard, P. Chang, Y. Chao, K.F. Chen, P.H. Chen, W.-S. Hou, Y.y. Li, R.-S. Lu, E. Paganis, A. Psallidas, A. Steen, E. Yazgan

Chulalongkorn University, Faculty of Science, Department of Physics, Bangkok, Thailand

B. Asavapibhop, C. Asawatangtrakuldee, N. Srimanobhas

Çukurova University, Physics Department, Science and Art Faculty, Adana, Turkey

M.N. Bakirci⁶⁰, F. Boran, S. Damarseckin⁶¹, Z.S. Demiroglu, F. Dolek, C. Dozen⁶², I. Dumanoglu⁶³, E. Eskut, G. Gokbulut, Y. Guler, E. Gurpinar Guler⁶⁴, I. Hos⁶⁵, C. Isik, E.E. Kangal⁶⁶, O. Kara, U. Kiminsu, G. Onengut, K. Ozdemir⁶⁷, A. Polatoz, A.E. Simsek, U.G. Tok, H. Topakli⁶⁸, S. Turkcapar, I.S. Zorbakir, C. Zorbilmez

Middle East Technical University, Physics Department, Ankara, Turkey

B. Isildak⁶⁹, G. Karapinar⁷⁰, K. Ocalan⁷¹, M. Yalvac⁷²

Bogazici University, Istanbul, Turkey

I.O. Atakisi, E. Gülmез, M. Kaya⁷³, O. Kaya⁷⁴, Ö. Özçelik, S. Tekten⁷⁵, E.A. Yetkin⁷⁶

Istanbul Technical University, Istanbul, Turkey

A. Cakir, K. Cankocak⁶³, Y. Komurcu, S. Sen⁷⁷

Istanbul University, Istanbul, Turkey

F. Aydogmus Sen, S. Cerci⁷⁸, B. Kaynak, S. Ozkorucuklu, D. Sunar Cerci⁷⁸

Institute for Scintillation Materials of National Academy of Science of Ukraine, Kharkov, Ukraine

B. Grynyov

National Scientific Center, Kharkov Institute of Physics and Technology, Kharkov, Ukraine

L. Levchuk

University of Bristol, Bristol, United Kingdom

E. Bhal, S. Bologna, J.J. Brooke, E. Clement, D. Cussans, H. Flacher, J. Goldstein, G.P. Heath, H.F. Heath, L. Kreczko, B. Krikler, S. Paramesvaran, T. Sakuma, S. Seif El Nasr-Storey, V.J. Smith, J. Taylor, A. Titterton

Rutherford Appleton Laboratory, Didcot, United Kingdom

K.W. Bell, A. Belyaev⁷⁹, C. Brew, R.M. Brown, D.J.A. Cockerill, K.V. Ellis, K. Harder,

S. Harper, J. Linacre, K. Manolopoulos, D.M. Newbold, E. Olaiya, D. Petyt, T. Reis, T. Schuh, C.H. Shepherd-Themistocleous, A. Thea, I.R. Tomalin, T. Williams

Imperial College, London, United Kingdom

R. Bainbridge, P. Bloch, S. Bonomally, J. Borg, S. Breeze, O. Buchmuller, A. Bundock, V. Cepaitis, G.S. Chahal⁸⁰, D. Colling, P. Dauncey, G. Davies, M. Della Negra, G. Fedi, G. Hall, G. Iles, J. Langford, L. Lyons, A.-M. Magnan, S. Malik, A. Martelli, V. Milosevic, J. Nash⁸¹, V. Palladino, M. Pesaresi, D.M. Raymond, A. Richards, A. Rose, E. Scott, C. Seez, A. Shtipliyski, M. Stoye, A. Tapper, K. Uchida, T. Virdee²⁰, N. Wardle, S.N. Webb, D. Winterbottom, A.G. Zecchinelli

Brunel University, Uxbridge, United Kingdom

J.E. Cole, P.R. Hobson, A. Khan, P. Kyberd, C.K. Mackay, I.D. Reid, L. Teodorescu, S. Zahid

Baylor University, Waco, USA

A. Brinkerhoff, K. Call, B. Caraway, J. Dittmann, K. Hatakeyama, A.R. Kanuganti, C. Madrid, B. McMaster, N. Pastika, S. Sawant, C. Smith

Catholic University of America, Washington, DC, USA

R. Bartek, A. Dominguez, R. Uniyal, A.M. Vargas Hernandez

The University of Alabama, Tuscaloosa, USA

A. Buccilli, O. Charaf, S.I. Cooper, S.V. Gleyzer, C. Henderson, P. Rumerio, C. West

Boston University, Boston, USA

A. Akpinar, A. Albert, D. Arcaro, C. Cosby, Z. Demiragli, D. Gastler, C. Richardson, J. Rohlf, K. Salyer, D. Sperka, D. Spitzbart, I. Suarez, S. Yuan, D. Zou

Brown University, Providence, USA

G. Benelli, B. Burkle, X. Coubez²¹, D. Cutts, Y.t. Duh, M. Hadley, U. Heintz, J.M. Hogan⁸², K.H.M. Kwok, E. Laird, G. Landsberg, K.T. Lau, J. Lee, M. Narain, S. Sagir⁸³, R. Syarif, E. Usai, W.Y. Wong, D. Yu, W. Zhang

University of California, Davis, Davis, USA

R. Band, C. Brainerd, R. Breedon, M. Calderon De La Barca Sanchez, M. Chertok, J. Conway, R. Conway, P.T. Cox, R. Erbacher, C. Flores, G. Funk, F. Jensen, W. Ko[†], O. Kukral, R. Lander, M. Mulhearn, D. Pellett, J. Pilot, M. Shi, D. Taylor, K. Tos, M. Tripathi, Y. Yao, F. Zhang

University of California, Los Angeles, USA

M. Bachtis, R. Cousins, A. Dasgupta, A. Florent, D. Hamilton, J. Hauser, M. Ignatenko, T. Lam, N. Mccoll, W.A. Nash, S. Regnard, D. Saltzberg, C. Schnaible, B. Stone, V. Valuev

University of California, Riverside, Riverside, USA

K. Burt, Y. Chen, R. Clare, J.W. Gary, S.M.A. Ghiasi Shirazi, G. Hanson, G. Karapostoli, O.R. Long, N. Manganelli, M. Olmedo Negrete, M.I. Paneva, W. Si, S. Wimpenny, Y. Zhang

University of California, San Diego, La Jolla, USA

J.G. Branson, P. Chang, S. Cittolin, S. Cooperstein, N. Deelen, M. Derdzinski, J. Duarte, R. Gerosa, D. Gilbert, B. Hashemi, V. Krutelyov, J. Letts, M. Masciovecchio, S. May, S. Padhi, M. Pieri, V. Sharma, M. Tadel, F. Würthwein, A. Yagil

University of California, Santa Barbara - Department of Physics, Santa Barbara, USA

N. Amin, C. Campagnari, M. Citron, A. Dorsett, V. Dutta, J. Incandela, B. Marsh, H. Mei, A. Ovcharova, H. Qu, M. Quinnan, J. Richman, U. Sarica, D. Stuart, S. Wang

California Institute of Technology, Pasadena, USA

D. Anderson, A. Bornheim, O. Cerri, I. Dutta, J.M. Lawhorn, N. Lu, J. Mao, H.B. Newman, T.Q. Nguyen, J. Pata, M. Spiropulu, J.R. Vlimant, S. Xie, Z. Zhang, R.Y. Zhu

Carnegie Mellon University, Pittsburgh, USA

J. Alison, M.B. Andrews, T. Ferguson, T. Mudholkar, M. Paulini, M. Sun, I. Vorobiev

University of Colorado Boulder, Boulder, USA

J.P. Cumalat, W.T. Ford, E. MacDonald, T. Mulholland, R. Patel, A. Perloff, K. Stenson, K.A. Ulmer, S.R. Wagner

Cornell University, Ithaca, USA

J. Alexander, Y. Cheng, J. Chu, D.J. Cranshaw, A. Datta, A. Frankenthal, K. Mcdermott, J. Monroy, J.R. Patterson, D. Quach, A. Ryd, W. Sun, S.M. Tan, Z. Tao, J. Thom, P. Wittich, M. Zientek

Fermi National Accelerator Laboratory, Batavia, USA

S. Abdullin, M. Albrow, M. Alyari, G. Apollinari, A. Apresyan, A. Apyan, S. Banerjee, L.A.T. Bauerdtick, A. Beretvas, D. Berry, J. Berryhill, P.C. Bhat, K. Burkett, J.N. Butler, A. Canepa, G.B. Cerati, H.W.K. Cheung, F. Chlebana, M. Cremonesi, V.D. Elvira, J. Freeman, Z. Gecse, E. Gottschalk, L. Gray, D. Green, S. Grünendahl, O. Gutsche, R.M. Harris, S. Hasegawa, R. Heller, T.C. Herwig, J. Hirschauer, B. Jayatilaka, S. Jindariani, M. Johnson, U. Joshi, P. Klabbers, T. Klijnsma, B. Klima, M.J. Kortelainen, S. Lammel, D. Lincoln, R. Lipton, M. Liu, T. Liu, J. Lykken, K. Maeshima, D. Mason, P. McBride, P. Merkel, S. Mrenna, S. Nahn, V. O'Dell, V. Papadimitriou, K. Pedro, C. Pena⁸⁴, O. Prokofyev, F. Ravera, A. Reinsvold Hall, L. Ristori, B. Schneider, E. Sexton-Kennedy, N. Smith, A. Soha, W.J. Spalding, L. Spiegel, S. Stoynev, J. Strait, L. Taylor, S. Tkaczyk, N.V. Tran, L. Uplegger, E.W. Vaandering, H.A. Weber, A. Woodard

University of Florida, Gainesville, USA

D. Acosta, P. Avery, D. Bourilkov, L. Cadamuro, V. Cherepanov, F. Errico, R.D. Field, D. Guerrero, B.M. Joshi, M. Kim, J. Konigsberg, A. Korytov, K.H. Lo, K. Matchev, N. Menendez, G. Mitselmakher, D. Rosenzweig, K. Shi, J. Wang, S. Wang, X. Zuo

Florida State University, Tallahassee, USA

T. Adams, A. Askew, D. Diaz, R. Habibullah, S. Hagopian, V. Hagopian, K.F. Johnson, R. Khurana, T. Kolberg, G. Martinez, H. Prosper, C. Schiber, R. Yohay, J. Zhang

Florida Institute of Technology, Melbourne, USA

M.M. Baarmann, S. Butalla, T. Elkafrawy¹², M. Hohlmann, D. Noonan, M. Rahmani, M. Saunders, F. Yumiceva

University of Illinois at Chicago (UIC), Chicago, USA

M.R. Adams, L. Apanasevich, H. Becerril Gonzalez, R. Cavanaugh, X. Chen, S. Dittmer, O. Evdokimov, C.E. Gerber, D.A. Hangal, D.J. Hofman, C. Mills, G. Oh, T. Roy, M.B. Tonjes, N. Varelas, J. Viinikainen, X. Wang, Z. Wu

The University of Iowa, Iowa City, USA

M. Alhusseini, K. Dilsiz⁸⁵, S. Durgut, R.P. Gandrajula, M. Haytmyradov, V. Khristenko, O.K. Köseyan, J.-P. Merlo, A. Mestvirishvili⁸⁶, A. Moeller, J. Nachtman, H. Ogul⁸⁷, Y. Onel, F. Ozok⁸⁸, A. Penzo, C. Snyder, E. Tiras, J. Wetzel, K. Yi⁸⁹

Johns Hopkins University, Baltimore, USA

O. Amram, B. Blumenfeld, L. Corcodilos, M. Eminizer, A.V. Gritsan, S. Kyriacou, P. Maksimovic, C. Mantilla, J. Roskes, M. Swartz, T.Á. Vámi

The University of Kansas, Lawrence, USA

C. Baldenegro Barrera, P. Baringer, A. Bean, A. Bylinkin, T. Isidori, S. Khalil, J. King, G. Krintiras, A. Kropivnitskaya, C. Lindsey, N. Minafra, M. Murray, C. Rogan, C. Royon, S. Sanders, E. Schmitz, J.D. Tapia Takaki, Q. Wang, J. Williams, G. Wilson

Kansas State University, Manhattan, USA

S. Duric, A. Ivanov, K. Kaadze, D. Kim, Y. Maravin, T. Mitchell, A. Modak, A. Mohammadi

Lawrence Livermore National Laboratory, Livermore, USA

F. Rebassoo, D. Wright

University of Maryland, College Park, USA

E. Adams, A. Baden, O. Baron, A. Belloni, S.C. Eno, Y. Feng, N.J. Hadley, S. Jabeen, G.Y. Jeng, R.G. Kellogg, T. Koeth, A.C. Mignerey, S. Nabili, M. Seidel, A. Skuja, S.C. Tonwar, L. Wang, K. Wong

Massachusetts Institute of Technology, Cambridge, USA

D. Abercrombie, B. Allen, R. Bi, S. Brandt, W. Busza, I.A. Cali, Y. Chen, M. D'Alfonso, G. Gomez Ceballos, M. Goncharov, P. Harris, D. Hsu, M. Hu, M. Klute, D. Kovalevskyi, J. Krupa, Y.-J. Lee, P.D. Luckey, B. Maier, A.C. Marini, C. McGinn, C. Mironov, S. Narayanan, X. Niu, C. Paus, D. Rankin, C. Roland, G. Roland, Z. Shi, G.S.F. Stephans, K. Sumorok, K. Tatar, D. Velicanu, J. Wang, T.W. Wang, Z. Wang, B. Wyslouch

University of Minnesota, Minneapolis, USA

R.M. Chatterjee, A. Evans, S. Guts[†], P. Hansen, J. Hiltbrand, Sh. Jain, M. Krohn, Y. Kubota, Z. Lesko, J. Mans, M. Revering, R. Rusack, R. Saradhy, N. Schroeder, N. Strobbe, M.A. Wadud

University of Mississippi, Oxford, USA

J.G. Acosta, S. Oliveros

University of Nebraska-Lincoln, Lincoln, USA

K. Bloom, S. Chauhan, D.R. Claes, C. Fangmeier, L. Finco, F. Golf, J.R. González Fernández, I. Kravchenko, J.E. Siado, G.R. Snow[†], B. Stieger, W. Tabb, F. Yan

State University of New York at Buffalo, Buffalo, USA

G. Agarwal, C. Harrington, L. Hay, I. Iashvili, A. Kharchilava, C. McLean, D. Nguyen, J. Pekkanen, S. Rappoccio, B. Roozbahani

Northeastern University, Boston, USA

G. Alverson, E. Barberis, C. Freer, Y. Haddad, A. Hortiangtham, J. Li, G. Madigan, B. Marzocchi, D.M. Morse, V. Nguyen, T. Orimoto, A. Parker, L. Skinnari, A. Tishelman-Charny, T. Wamorkar, B. Wang, A. Wisecarver, D. Wood

Northwestern University, Evanston, USA

S. Bhattacharya, J. Bueghly, Z. Chen, A. Gilbert, T. Gunter, K.A. Hahn, N. Odell, M.H. Schmitt, K. Sung, M. Velasco

University of Notre Dame, Notre Dame, USA

R. Bucci, N. Dev, R. Goldouzian, M. Hildreth, K. Hurtado Anampa, C. Jessop, D.J. Karmgard, K. Lannon, W. Li, N. Loukas, N. Marinelli, I. McAlister, F. Meng, K. Mohrman, Y. Musienko⁴⁵, R. Ruchti, P. Siddireddy, S. Taroni, M. Wayne, A. Wightman, M. Wolf, L. Zygala

The Ohio State University, Columbus, USA

J. Alimena, B. Bylsma, B. Cardwell, L.S. Durkin, B. Francis, C. Hill, A. Lefeld, B.L. Winer, B.R. Yates

Princeton University, Princeton, USA

P. Das, G. Dezoort, P. Elmer, B. Greenberg, N. Haubrich, S. Higginbotham, A. Kalogeropoulos, G. Kopp, S. Kwan, D. Lange, M.T. Lucchini, J. Luo, D. Marlow, K. Mei, I. Ojalvo, J. Olsen, C. Palmer, P. Piroué, D. Stickland, C. Tully

University of Puerto Rico, Mayaguez, USA

S. Malik, S. Norberg

Purdue University, West Lafayette, USA

V.E. Barnes, R. Chawla, S. Das, L. Gutay, M. Jones, A.W. Jung, B. Mahakud, G. Negro, N. Neumeister, C.C. Peng, S. Piperov, H. Qiu, J.F. Schulte, N. Trevisani, F. Wang, R. Xiao, W. Xie

Purdue University Northwest, Hammond, USA

T. Cheng, J. Dolen, N. Parashar, M. Stojanovic

Rice University, Houston, USA

A. Baty, S. Dildick, K.M. Ecklund, S. Freed, F.J.M. Geurts, M. Kilpatrick, A. Kumar, W. Li, B.P. Padley, R. Redjimi, J. Roberts[†], J. Rorie, W. Shi, A.G. Stahl Leiton

University of Rochester, Rochester, USA

A. Bodek, P. de Barbaro, R. Demina, J.L. Dulemba, C. Fallon, T. Ferbel, M. Galanti, A. Garcia-Bellido, O. Hindrichs, A. Khukhunaishvili, E. Ranken, R. Taus

Rutgers, The State University of New Jersey, Piscataway, USA

B. Chiarito, J.P. Chou, A. Gandrakota, Y. Gershtein, E. Halkiadakis, A. Hart, M. Heindl, E. Hughes, S. Kaplan, O. Karacheban²⁴, I. Laflotte, A. Lath, R. Montalvo, K. Nash, M. Osherson, S. Salur, S. Schnetzer, S. Somalwar, R. Stone, S.A. Thayil, S. Thomas, H. Wang

University of Tennessee, Knoxville, USA

H. Acharya, A.G. Delannoy, S. Spanier

Texas A&M University, College Station, USA

O. Bouhali⁹⁰, M. Dalchenko, A. Delgado, R. Eusebi, J. Gilmore, T. Huang, T. Kamon⁹¹, H. Kim, S. Luo, S. Malhotra, R. Mueller, D. Overton, L. Perniè, D. Rathjens, A. Safonov, J. Sturdy

Texas Tech University, Lubbock, USA

N. Akchurin, J. Damgov, V. Hegde, S. Kunori, K. Lamichhane, S.W. Lee, T. Mengke, S. Muthumuni, T. Peltola, S. Undleeb, I. Volobouev, Z. Wang, A. Whitbeck

Vanderbilt University, Nashville, USA

E. Appelt, S. Greene, A. Gurrola, R. Janjam, W. Johns, C. Maguire, A. Melo, H. Ni, K. Padeken, F. Romeo, P. Sheldon, S. Tuo, J. Velkovska, M. Verweij

University of Virginia, Charlottesville, USA

M.W. Arenton, B. Cox, G. Cummings, J. Hakala, R. Hirosky, M. Joyce, A. Ledovskoy, A. Li, C. Neu, B. Tannenwald, Y. Wang, E. Wolfe, F. Xia

Wayne State University, Detroit, USA

P.E. Karchin, N. Poudyal, P. Thapa

University of Wisconsin - Madison, Madison, WI, USA

K. Black, T. Bose, J. Buchanan, C. Caillol, S. Dasu, I. De Bruyn, P. Everaerts, C. Galloni,

H. He, M. Herndon, A. Hervé, U. Hussain, A. Lanaro, A. Loeliger, R. Loveless,
J. Madhusudanan Sreekala, A. Mallampalli, D. Pinna, T. Ruggles, A. Savin, V. Shang, V. Sharma,
W.H. Smith, D. Teague, S. Trembath-reichert, W. Vetens

†: Deceased

- 1: Also at Vienna University of Technology, Vienna, Austria
- 2: Also at Institute of Basic and Applied Sciences, Faculty of Engineering, Arab Academy for Science, Technology and Maritime Transport, Alexandria, Egypt, Alexandria, Egypt
- 3: Also at Université Libre de Bruxelles, Bruxelles, Belgium
- 4: Also at IRFU, CEA, Université Paris-Saclay, Gif-sur-Yvette, France
- 5: Also at Universidade Estadual de Campinas, Campinas, Brazil
- 6: Also at Federal University of Rio Grande do Sul, Porto Alegre, Brazil
- 7: Also at UFMS, Nova Andradina, Brazil
- 8: Also at Universidade Federal de Pelotas, Pelotas, Brazil
- 9: Also at University of Chinese Academy of Sciences, Beijing, China
- 10: Also at Institute for Theoretical and Experimental Physics named by A.I. Alikhanov of NRC 'Kurchatov Institute', Moscow, Russia
- 11: Also at Joint Institute for Nuclear Research, Dubna, Russia
- 12: Also at Ain Shams University, Cairo, Egypt
- 13: Also at Suez University, Suez, Egypt
- 14: Now at British University in Egypt, Cairo, Egypt
- 15: Now at Cairo University, Cairo, Egypt
- 16: Also at Purdue University, West Lafayette, USA
- 17: Also at Université de Haute Alsace, Mulhouse, France
- 18: Also at Tbilisi State University, Tbilisi, Georgia
- 19: Also at Erzincan Binali Yıldırım University, Erzincan, Turkey
- 20: Also at CERN, European Organization for Nuclear Research, Geneva, Switzerland
- 21: Also at RWTH Aachen University, III. Physikalisches Institut A, Aachen, Germany
- 22: Also at University of Hamburg, Hamburg, Germany
- 23: Also at Department of Physics, Isfahan University of Technology, Isfahan, Iran, Isfahan, Iran
- 24: Also at Brandenburg University of Technology, Cottbus, Germany
- 25: Also at Skobeltsyn Institute of Nuclear Physics, Lomonosov Moscow State University, Moscow, Russia
- 26: Also at Institute of Physics, University of Debrecen, Debrecen, Hungary, Debrecen, Hungary
- 27: Also at Physics Department, Faculty of Science, Assiut University, Assiut, Egypt
- 28: Also at MTA-ELTE Lendület CMS Particle and Nuclear Physics Group, Eötvös Loránd University, Budapest, Hungary, Budapest, Hungary
- 29: Also at Institute of Nuclear Research ATOMKI, Debrecen, Hungary
- 30: Also at IIT Bhubaneswar, Bhubaneswar, India, Bhubaneswar, India
- 31: Also at Institute of Physics, Bhubaneswar, India
- 32: Also at G.H.G. Khalsa College, Punjab, India
- 33: Also at Shoolini University, Solan, India
- 34: Also at University of Hyderabad, Hyderabad, India
- 35: Also at University of Visva-Bharati, Santiniketan, India
- 36: Also at Indian Institute of Technology (IIT), Mumbai, India
- 37: Also at Deutsches Elektronen-Synchrotron, Hamburg, Germany
- 38: Also at Department of Physics, University of Science and Technology of Mazandaran, Behshahr, Iran

- 39: Now at INFN Sezione di Bari ^a, Università di Bari ^b, Politecnico di Bari ^c, Bari, Italy
40: Also at Italian National Agency for New Technologies, Energy and Sustainable Economic Development, Bologna, Italy
41: Also at Centro Siciliano di Fisica Nucleare e di Struttura Della Materia, Catania, Italy
42: Also at Riga Technical University, Riga, Latvia, Riga, Latvia
43: Also at Consejo Nacional de Ciencia y Tecnología, Mexico City, Mexico
44: Also at Warsaw University of Technology, Institute of Electronic Systems, Warsaw, Poland
45: Also at Institute for Nuclear Research, Moscow, Russia
46: Now at National Research Nuclear University 'Moscow Engineering Physics Institute' (MEPhI), Moscow, Russia
47: Also at Institute of Nuclear Physics of the Uzbekistan Academy of Sciences, Tashkent, Uzbekistan
48: Also at St. Petersburg State Polytechnical University, St. Petersburg, Russia
49: Also at University of Florida, Gainesville, USA
50: Also at Imperial College, London, United Kingdom
51: Also at P.N. Lebedev Physical Institute, Moscow, Russia
52: Also at Budker Institute of Nuclear Physics, Novosibirsk, Russia
53: Also at Faculty of Physics, University of Belgrade, Belgrade, Serbia
54: Also at Trincomalee Campus, Eastern University, Sri Lanka, Nilaveli, Sri Lanka
55: Also at INFN Sezione di Pavia ^a, Università di Pavia ^b, Pavia, Italy, Pavia, Italy
56: Also at National and Kapodistrian University of Athens, Athens, Greece
57: Also at Universität Zürich, Zurich, Switzerland
58: Also at Stefan Meyer Institute for Subatomic Physics, Vienna, Austria, Vienna, Austria
59: Also at Laboratoire d'Annecy-le-Vieux de Physique des Particules, IN2P3-CNRS, Annecy-le-Vieux, France
60: Also at Gaziosmanpasa University, Tokat, Turkey
61: Also at Şırnak University, Şırnak, Turkey
62: Also at Department of Physics, Tsinghua University, Beijing, China, Beijing, China
63: Also at Near East University, Research Center of Experimental Health Science, Nicosia, Turkey
64: Also at Beykent University, Istanbul, Turkey, Istanbul, Turkey
65: Also at Istanbul Aydin University, Application and Research Center for Advanced Studies (App. & Res. Cent. for Advanced Studies), Istanbul, Turkey
66: Also at Mersin University, Mersin, Turkey
67: Also at Piri Reis University, Istanbul, Turkey
68: Also at Tarsus University, MERSIN, Turkey
69: Also at Ozyegin University, Istanbul, Turkey
70: Also at Izmir Institute of Technology, Izmir, Turkey
71: Also at Necmettin Erbakan University, Konya, Turkey
72: Also at Bozok Universitetesi Rektörlüğü, Yozgat, Turkey, Yozgat, Turkey
73: Also at Marmara University, Istanbul, Turkey
74: Also at Milli Savunma University, Istanbul, Turkey
75: Also at Kafkas University, Kars, Turkey
76: Also at Istanbul Bilgi University, Istanbul, Turkey
77: Also at Hacettepe University, Ankara, Turkey
78: Also at Adiyaman University, Adiyaman, Turkey
79: Also at School of Physics and Astronomy, University of Southampton, Southampton, United Kingdom
80: Also at IPPP Durham University, Durham, United Kingdom

- 81: Also at Monash University, Faculty of Science, Clayton, Australia
- 82: Also at Bethel University, St. Paul, Minneapolis, USA, St. Paul, USA
- 83: Also at Karamanoğlu Mehmetbey University, Karaman, Turkey
- 84: Also at California Institute of Technology, Pasadena, USA
- 85: Also at Bingol University, Bingol, Turkey
- 86: Also at Georgian Technical University, Tbilisi, Georgia
- 87: Also at Sinop University, Sinop, Turkey
- 88: Also at Mimar Sinan University, Istanbul, Istanbul, Turkey
- 89: Also at Nanjing Normal University Department of Physics, Nanjing, China
- 90: Also at Texas A&M University at Qatar, Doha, Qatar
- 91: Also at Kyungpook National University, Daegu, Korea, Daegu, Korea